Technical University of Denmark

DTU

Load alleviation potential of the Controllable Rubber Trailing Edge Flap (CRTEF) in the INDUFLAP project

Barlas, Athanasios; Bergami, Leonardo; Hansen, Morten Hartvig; Pedersen, Mads Mølgaard; Thomsen, Kenneth; Aagaard Madsen , Helge

DTU Library
Technical Information Center of Denmark

Load alleviation potential of the Controllable Rubber Trailing Edge Flap (CRTEF) in the INDUFLAP project

Thanasis K. Barlas, Leonardo Bergami, Morten H. Hansen, Mads M. Pedersen, David Verelst, Kenneth Thomsen, Helge A. Madsen

DTU Vindenergi
Institut for Vindenergi
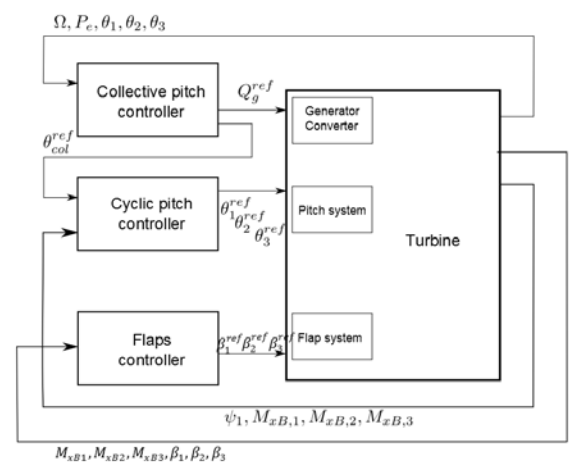
Authors: Thanasis K. Barlas, Leonardo Bergami, Morten H. Hansen, Mads M. Pedersen, Kenneth Thomsen, Helge A. Madsen

Title: Load alleviation potential of the Controllable Trailing Edge Flap (CRTEF) in the INDUFLAP project.

Summary (max 2000 characters):
The load alleviation potential of the Controllable Rubber Trailing Edge Flap (CRTEF) is verified on a full Design Load Base (DLB) setup using the aeroelastic code HAWC2, and by investigating a flap configuration for the NREL 5MW Reference Wind Turbine (RWT) model. The performance of the CRTEF configuration are first compared against the ones obtained with individual pitch control ; a third configuration is also investigated, where CRTEF and individual pitch controller are combined. The CRTEF allows for a significant reduction of the lifetime fatigue on various load channels; the reduction for some of the extreme loads is also noticeable

Preface

The report describes the aeroelastic simulation activities on the load alleviation potential of a trailing edge flap in a realistic setup, close to the industrial certification-type of simulations. The implementation, load basis and pre-/post-processing comprise a robust and concrete comparison of load alleviation concepts.

Roskilde, December 2014

Thanasis K. Barlas
Researcher

Content

Summary

The load alleviation potential of the Controllable Rubber Trailing Edge Flap (CRTEF) is verified on a full Design Load Base (DLB) setup using the aeroelastic code HAWC2, and by investigating a flap configuration for the NREL 5MW Reference Wind Turbine (RWT) model. The performance of the CRTEF configuration are first compared against the ones obtained with individual pitch control ; a third configuration is also investigated, where CRTEF and individual pitch controller are combined. The CRTEF allows for a significant reduction of the lifetime fatigue on various load channels; the reduction for some of the extreme loads is also noticeable.

1. Introduction, background and objectives

In this section, the current evaluation of the flap load alleviation potential is introduced, together with background information and general objectives in the context of the INDUFLAP project.

Introduction

Testing the performance and robustness of the smart blade technology is an important part of the INDUFLAP project. Wind tunnel testing of an earlier prototype flap system was performed in 2009 and proved that the actuation concept works in a wind tunnel [1, 2]. The rotating rig testing of the latest prototype developed in the project is documented in [3, 4]. However, a big step from prototype testing to full scale turbine application is a realistic evaluation of the load alleviation potential of such a system in conditions close to industrial standards.

Background information

The load alleviation potential of using active flaps on wind turbine rotors has been investigated in the past decade using various models, controllers, configurations and load cases. For an overview see [5]. In this report, the aeroelastic load simulations present a first approach for documenting such an evaluation on an overall realistic setup.

Main characteristics of the simulations:
- Certification-type design load base setup close to industrial standards
- Representative wind turbine / flap system configuration
- Realistic controllers for full range of operation

2. The full Design Load Base (DLB) setup

This section briefly describes the full Design Load Basis (DLB) used for load calculations at DTU Wind Energy for onshore wind turbines. This setup is used in the presented load evaluation of the flap system. A detailed description of the DLB is found in [**6**].

DLB setup

In order to assess the load consequences of innovative features and devices added to existing wind turbine concepts or new developed wind turbine design concepts, it is useful to have a full DLB that follows the current design standard and is representative of a general DLB used by the industry in a certification process. The proposed DLB is based on the third edition of the IEC 61400-1 standard [**7**] and covers the typical cases for assessment of extreme and fatigue loads on the turbine components. The overview of the parameters defining the Design Load Cases (DLC) is presented in **Table 1**. In the table, the name of the DLC according to IEC is mentioned, together with the type of load analysis (U=extreme/ultimate loads and F=fatigue) and the partial safety factor on the loads. A short description of the operating conditions is also added, including the details for the range of mean wind speeds at hub height, the mean yaw errors in degrees, the turbulence model or turbulence intensity used, the number of turbulence seeds used per wind speed and yaw error, the vertical shear exponent, the gust type, the short description of fault type, the length of simulated load signal used for analysis in seconds and the number of resulting files.

Generally, the wind speed range for normal operation is here set to 4 – 26 m/s and all simulations performed with an aerodynamic and mass imbalance on the blades. The results of DLCs 1.2, 2.4, 3.1, 4.1, and 6.4 are utilized for fatigue calculations, while the results of DLC 1.2 are used for estimation of the maximum 50-year occurrence loads using statistical extrapolation. DLC 7.1 (locked rotor with extreme yaw), which appears in the IEC standard has been disregarded, due to problematic implementation with the current capabilities of the aeroelastic tool. The suggested implementation of the DLCs is considered accurate translation of the IEC recommendation and a good choice for research investigation, close to certification-type of load analysis.

Table 1 - Overview of the DLB parameters.

Name	Load	PSF	Description	WSP	Wdir	Turb	Seeds	Shear	Gust	Fault	DLC_dist	WSP_dist	Wdir_dist	T
DLCxxx	U: ultimate, F: fatigue	Partial safety factor for U		Wind speed [m/s]	Wind direction [deg]	Turbulence	Number of seeds	Shear factor	None, EDC, NTM		Fatige DLC distribution [xx=>xx%], [#xx=>xx pr year]	Fatigue WSP distribution [xx=>xx% or #xx=>xx pr year]	Fatige Wdir distribution [%]	Simulation time [s]
DLC12	U/F	1.25	Normal production	4:2:26	-10/0/10	NTM	6	0.2	None	None	97.5	Weibull	25/50/25	600
DLC13	U	1.35	Normal production	4:2:26	-10/0/10	ETM	2	0.2	None	None				600
DLC14	U	1.35	Normal production	Vr/Vr+2/Vr-2	0	None	None	0.2	ECD	None				100
DLC15	U	1.35	Normal production	4:2:26	0	None	None	Eq. in IEC	EWS	None				100
DLC21	U	1.35	Grid loss	4:2:26	-10/0/10	NTM	4	0.2	None	Grid loss at 10s				100
DLC22y	U	1.1	Extreme yaw error	4:2:26	15:15:75/285:15:345	NTM	1	0.2	None	Abnormal yaw error				600
DLC22b	U	1.1	One blade stuck at min. angle	4:2:26	0	NTM	12	0.2	None	1 blade at fine pitch				600
DLC23	U	1.1	Grid loss	Vr+2/Vr-2/Vout	0	None	None	0.2	EOG	Grid loss at three diff. times				100
DLC24	U/F	1.35	Production in large yaw error	4:2:26	-20/20	NTM	3	0.2	None	Large yaw error	0.57	Weibull	50/50	600
DLC31	F	1.0	Start-up	Vin/Vr/Vout	0	None	None	0.2	None	None	0.872	90.91/4.55/4.55	100	250
DLC32	U	1.35	Start-up at four diff. times	Vin/Vr+2/Vr-2/Vout	0	None	None	0.2	EOG	None				100
DLC33	U	1.35	Start-up in EDC	Vin/Vr+2/Vr-2/Vout	0	None	None	0.2	EDC	None				100
DLC41	F	1.0	Shut-down	Vin/Vr/Vout	0	None	None	0.2	None	None	0.872	90.91/4.55/4.55	100	250
DLC42	U	1.35	Shut-down at six diff. times	Vr+2/Vr-2/Vout	0	None	None	0.2	EOG	None				100
DLC51	U	1.35	Emergency shut-down	Vr+2/Vr-2/Vout	0	NTM	12	0.2	None	None				100
DLC61	U	1.35	Parked in extreme wind	V50	-8/8	0.11	6	0.11	None	None				600
DLC62	U	1.1	Parked grid loss	V50	0:15:345	0.11	1	0.11	None	None				600
DLC63	U	1.35	Parked with large yaw error	V1	-20/20	0.11	6	0.11	None	None				600
DLC64	F	1.0	Parked	4:2:0.7*Vref	-8/8	NTM	7	0.2	None	None	2.5	Weibull	50/50	600
DLC81	U	1.5	Maintenance	Vmaint	-8/8	NTM	6	0.2	None	Maintenance				600
		Totals									102.314			159.8055556

For cases with flap controls, the standard list of DLCs is augmented with some additional cases, simulating reference fault cases related to the flap system (**Table 2**).

Table 2 - Flap fault cases.

Name	Load	PSF	Description	WSP	Wdir	Turb	Seeds	Shear	Gust	Fault	DLC_dist	WSP_dist	Wdir_dist	T	Files
DLCxxx	U: ultimate, F: fatigue	Partial safety factor for U		Wind speed [m/s]	Wind direction [deg]	Turbulence	Number of seeds	Shear factor	None, EDC, NTM		Fatige DLC distribution [xx=>xx%], [#xx=>xx pr year]	Fatige WSP distribution [xx=>xx% or #xx=>xx pr year]	Fatige Wdir distribution [%]	Simulation time [s]	Number of files
DLC22f1	U	1.1	Flap runaway symmetric	12:2:26	0	NTM	12	0.2	None	Sym Flap runaway to max defl				100	96
DLC22f2	U	1.1	Flap runaway asymm	12:2:26	0	NTM	12	0.2	None	Asym Flap runaway to max defl				100	96
DLC22f3	U	1.1	Flap actuator large delay	12:2:26	0	NTM	12	0.2	None	Flap act time const x5				100	96

Pre-/post processing

The standard DTU Wind Energy Design Load Case post-processing method for the DLB has been utilized. The pre-processing tools are available in [**8**].Thhis procedure and algorithms applied are described in detail in [**9**]. This includes the process of extraction of the defined load sensors statistics, the ultimate (extreme value) analysis including the prescribed safety factor, and the fatigue analysis. Representative load sensors on the main components of the wind turbine aeroelastic model are chosen, with the corresponding parameters for fatigue analysis shown in **Table 3**. The pitch bearing damage is also calculated, together with the pitch and flap activity.

Table 3 - Load sensor channel parameters

Name	Description	Nr	Unit	Statistic	Ultimate	Fatigue	M	NeqL	BearingDamage	MinDistance
MxTB	Tower bottom fore-aft	17	kNm		x	x	4	1E+07		
MyTB	Tower bottom side-side	18	kNm		x	x	4	1E+07		
MxTT	Tower top tilt	20	kNm		x	x	4	1E+07		
MyTT	Tower top roll	21	kNm		x	x	4	1E+07		
MzTT	Tower top yaw	22	kNm		x	x	4	1E+07		
MxMB	Main bearing tilt	23	kNm		x	x	4	1E+07		
MyMB	Main bearing yaw	24	kNm		x	x	4	1E+07		
MzMB	Main bearing torsion	25	kNm		x	x	4	1E+07		
MxBR	Blade root flap	(26,32,38)	kNm		x	x	10	1E+07		
MyBR	Blade root edge	(27,33,39)	kNm		x	x	10	1E+07		
MzBR	Blade root torsion	(28,34,40)	kNm		x	x	10	1E+07		
Power	Electrical power	90	W	x						
RPM	Rotational speed	3	rpm	x						
Pitch	Pitch angle	(4,6,8)	deg	x						
FlapActiv	Flap Activity	((103, 102), (104, 102), (105, 102))	deg				1	3E+06	x	
PitchActiv	Pitch Bearing Activity	((4, 102), (6, 102), (8, 102))	deg				1	3E+06	x	
PitchBear	Pitch Bearing Damage	((4, 26), (6, 32), (8, 38))					3	1	x	
TTDist	Distance from blade tips to tow	((50,51,52), (62,63,64), (65,66,67), (68,69,70))	m							13.448

In addition, the extrapolation of extreme loads from cases DLC1.2 is performed to statistically determine the long term load extremes [**10**].

3. Wind turbine model configuration

In this section the simulated wind turbine model is described, together with the characteristics of the implemented flap system.

Wind turbine model

The NREL 5MW Reference Wind Turbine (RWT) [**11**] is used for the simulations in the aeroelastic code HAWC2 [**12**], as a representative modern multi-MW wind turbine model which has been used extensively for comparison studies involving blade aerodynamic controls. The main geometrical and operational properties of the reference wind turbine are shown in **Table 4**. In this investigation, the IEC class has been changed from originally used IB to IA for evaluation of the load reduction potential in more aggressive wind conditions.

Table 4 - Main parameters of the NREL 5MW RWT.

NREL 5MW Reference Wind Turbine	
Rated power	5 MW
Number of blades	3
Rotor diameter	126 m
Blade length	61.5 m
Hub height	90 m
Overhang, tilt, precone	5m, 5°, 2.5^o
Rated rotor speed	1.267 rad/s
Rated wind speed	11.4 m
Cut-in, cut-out wind speed	3 m/s, 25 m/s
Baseline controller	Variable speed, pitch regulation
IEC class	IA

Flaps modelling

The simulated flap configuration is chosen based on prior studies [**12**] and enlarged (from originally 20%) to 30% of the blade length (**Figure 1**), in order to explore a more extended flap configuration (**Table 5**).

Table 5 - Flap parameters.

ATEF flap configuration	
Chordwise extension	10%
Deflection angle limits	$\pm 10^o$
Spanwise length	17.8m (29% blade length)
Spanwise location	43.05m-60.88m (from blade root)
Airfoil	NACA64618
Max ΔC_l	0.4
Deflection rate limit	100°/s
Actuator time constant	100ms

The unsteady aerodynamics associated with the active flaps is accounted for by using the ATEFlap dynamic stall model in HAWC2 [**13, 14**]. The variation of steady lift, drag, and moment coefficients introduced by the flap deflection in based on 2D CFD simulations performed with the code Ellipsys2D [**15**]. The exact shape of the deformed flap is shown in **Figure 2** and **Figure 3**. The flap structural dynamics are not accounted for in HAWC2, assuming a small flap and actuator size and weight, and not coupling with the rest of the blade structure. The actuator dynamics are implemented as a linear servo model in HAWC2, for a first order system with a time constant of 0.1s. This corresponds to the characteristics of a Controllable Rubber Trailing Edge Flap (CRTEF) actuator.
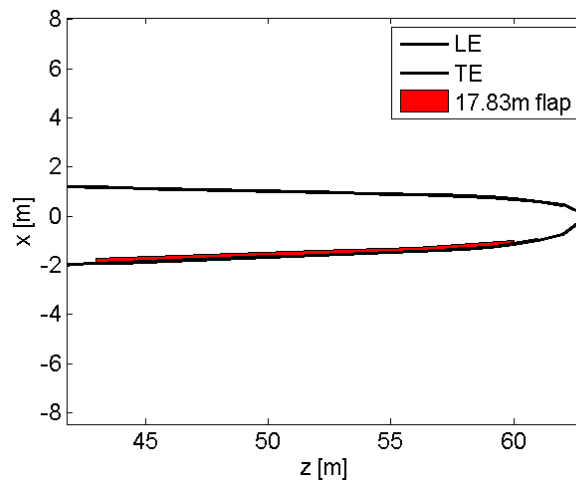

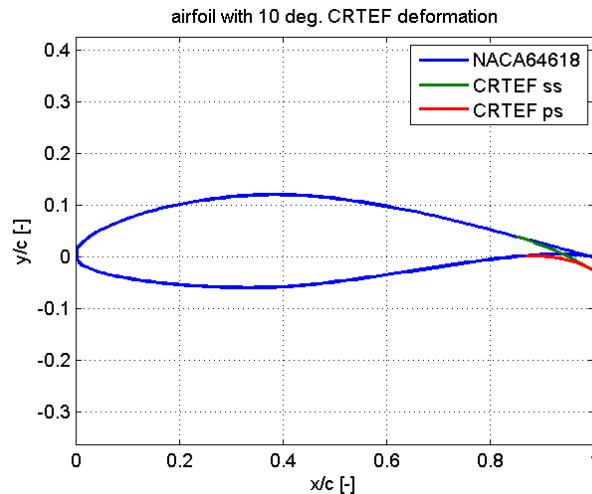**Figure 1 - Flap geometry implemented on the 61.5m blade of the NREL 5MW RWT.**

Figure 2 - NACA64618 geometry with a 10%c flap (10° positive flap deflection).
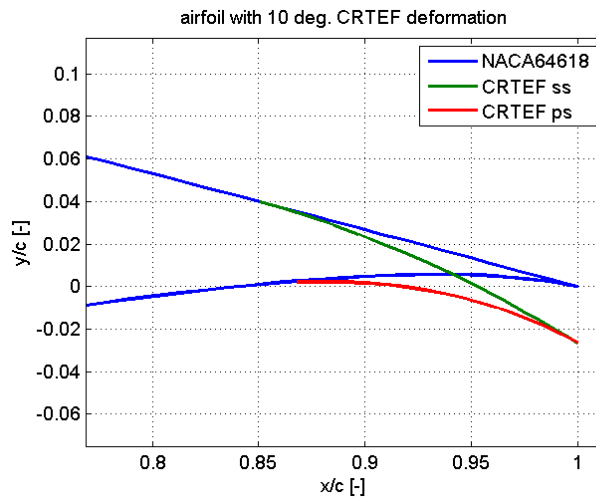
Figure 3 – NACA64618 geometry with a 10%c flap (10° positive flap deflection) (zoom in).

4. Controllers

In this section the implemented controllers are described.

Baseline controller

The baseline controller of the NREL 5MW RWT is originally described in [**10**]. Due to the fact that the original controller is not designed to handle operation in the full IEC DLCs, the basic DTU wind energy controller is used as described in [**16**]. The controller features both partial and full load operation as well as switching mechanisms between modes of operation, utilizing measurements of rotor speed, tower accelerations and pitch angles as inputs and the generator torque and collective pitch angle as outputs. Gain scheduling is employed for the pitch angle in full load operation. Furthermore, the controller includes procedures for cut-in, cut-out, overspeed and tower acceleration. A servo model for the pitch actuator is also included, as described in [**16**]. Finally, fault procedures for handling the relevant IEC fault cases are included. The top-level controller schematic is shown in **Figure 4**.
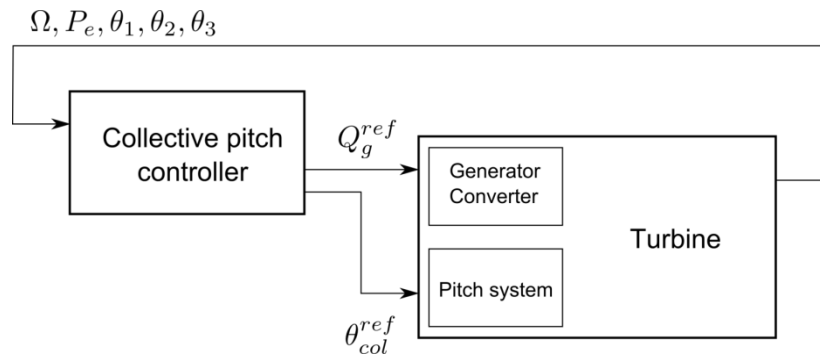

Figure 4 - Baseline controller.

Individual pitch controller

The individual pitch control is added on top of the baseline controller based on [**17**]. It utilizes flapwise blade root bending moment signals and azimuth position to control the individual pitch angles. The details of the controller are shown in the schematic in **Figure 6**. The root moments are transformed to the fixed reference frame resulting in two signals representing the rotor yaw and tilt moments; the rotor tilt and yaw signals are filtered with a low pass and a notch filter that excludes the 3P frequency; two PI loops are then applied to the filtered moment signals. The resulting pitch control signals are then transformed back to the rotating frame by adding a lead angle to the azimuthal position of each of the three blades; the pitch variation from the individual control is superimposed to the collective blade pitch angle. The individual pitch controller is tuned using a similar Ziegler-Nichols based scheme as used for the flap controller described in the next section.
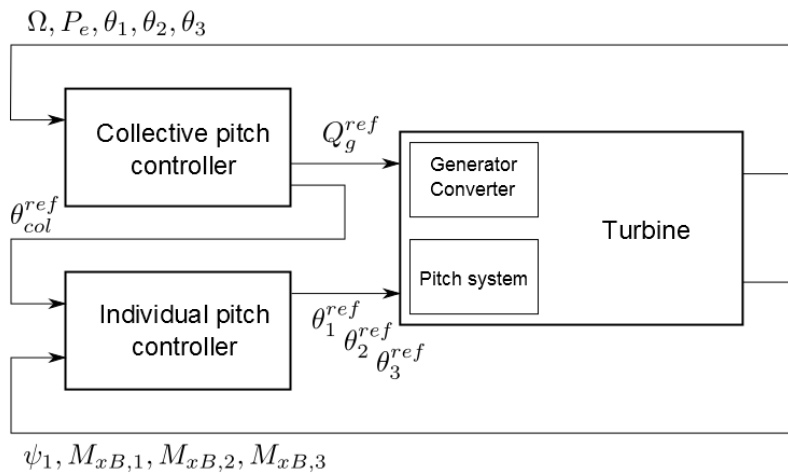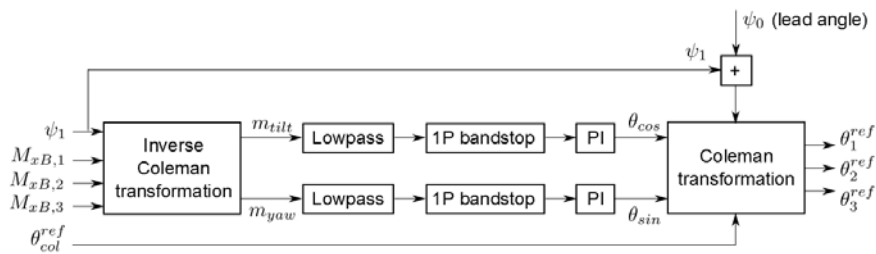
Figure 5 - Individual pitch controller.

Figure 6 - Details of the individual pitch controller.

Flap controller

Prior studies have explored advanced flap controllers together with various design configurations. In this study a simple flap controller close to industry standards is chosen, which can also operate at the full DLB, in a realistic setup.

The flap control algorithm drives the flap on each of the blade independently from the other. For each blade, the input to the flap control algorithm is the blade root bending moment in the flapwise direction and the output is the deflection of the flap on the same blade, accounting for delays and limitations of the flap actuator. The blade root flapwise bending moments are first high-pass filtered, as the flap should not compensate for the steady and low frequency variations. The reference flap signal is then proportional to the filtered bending moment and its first time derivative (PD control). The gains are scheduled as linear functions of the mean pitch angle, and an additional gain scheduling is introduced to limit the flap activity below rated power. To account for the actuator physical limitations, the reference flap signal is saturated within the range of allowed deflection, and for the maximum deflection rate. The actuators dynamics are then modelled as a first order low pass filter. The flap controller is not active in partial load operation or fault cases. The top level schematic of the controller is shown in **Figure 7.**
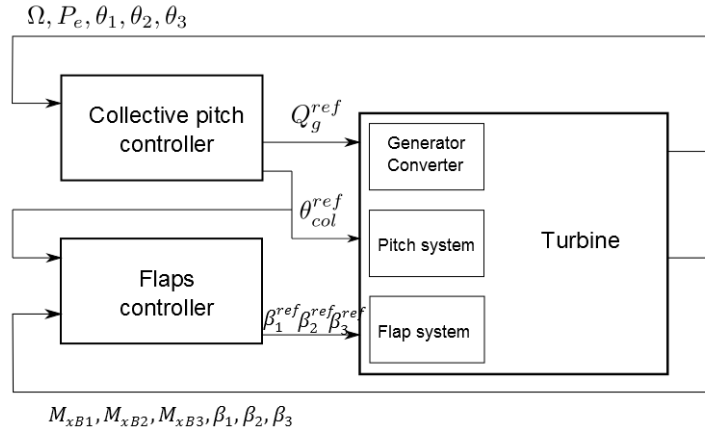
Figure 7 - Flaps controller.

The details of the Flap controller are shown in **Figure 8**. The process of the algorithm is summarized as follows:

- A high-pass filter is applied on the blade root flapwise bending moment output. The filter corner frequency is set to 0.05 Hz.
- Linear scheduling of the gains is applied based on low-passed filter averaged pitch signal $\bar{\theta}$ from the main controller (**Eq. 1**), where the linear scheduling factors k_{KP} k_{KD}, and the reference tuning gains k_P^{ref} k_D^{ref} are described later on.

$$k_P = k_P^{ref} + k_{KP}(\bar{\theta} - \theta^{ref})$$
$$k_D = k_D^{ref} + k_{KP}(\bar{\theta} - \theta^{ref}) \quad \textbf{(Eq. 1)}$$

- To limit the operation of the flaps below rated power, and achieve a smooth transition between below and above rated power operation, the flap control gains are all scaled by a factor k_{rp} with a linear dependence on the switch signal s_{rp} returned by the main controller. The switch signal is a low-pass filtered indicator of whether the turbine is operating at rated power ($s_{rp} = 1$) or not ($s_{rp} = 0$). To increase the flap activity, and hence load reduction in the transition region, a user specified threshold of the switch signal s_{rp}^{inp} is introduced; above the threshold, full gains are used ($s_{rp} = 1$), while below, a linear scaling to zero is applied ($k_{rp} = \frac{s_{rp}}{s_{rp}^{inp}}$).

- The reference flap signal for each of the blade is then proportional to the high-pass filtered blade root bending moment, and its first time derivative. The scheduled controller gains are also multiplied by the rated-power scaling factor k_{rp} (**Eq. 2**).

$$\beta_{ref} = k_{rp} \cdot (k_P \cdot M_x^f + k_D \cdot \frac{dM_x^f}{dt}) \quad \textbf{(Eq. 2)}$$

- To account for the physical limitations of the actuator, the reference flap signal is first saturated between maximum and minimum deflection, and then saturated for maximum flap deflection rate.
- The saturated reference flap signal then undergoes a first order low pass filter, which represents the physical actuators dynamics.
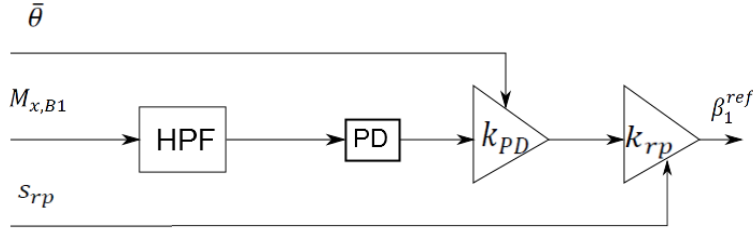
Figure 8 - Details of the flap controller.

The PD flap controller gains are tuned based on the response of a high-fidelity linear aero-servo-elastic model of the turbine and its controllers, obtained with HAWCStab2 [18]. HAWCStab2 returns a linearized high order state-space description of the turbine in an open-loop configuration at different operating points, as well as state-space matrices for the linearized collective power control. For a simplified tuning procedure, the three individual flap controllers are simply approximated as a single PD controller of the symmetric collective flap actions, based on a feedback of the variations in the collective blade root flapwise bending moment. A closed loop description that includes both power and flap control, returns then an indication of the stability for the complete aero-servo-elastic linear system.

The gains for the PD flap controllers are found with a Ziegler-Nichols tuning method. The gain on the derivative term is set to zero, whereas the proportional term gain is increased until a pole of the closed loop aero-servo-elastic system becomes unstable (**Figure 9**). The gain at which the pole becomes unstable is the critical gain k_k and f_k the pole frequency. The PD controller gains are then set to $k_P = 0.6 \cdot k_k$ and $k_d = 0.125 \cdot k_P \cdot f_k^{-1}$.

The linearized closed-loop system representation of the flap control is rather approximate, as it neglects the limits on the flap deflection range, the flap actuator dynamics, the high-pass filter on the bending moment measurement, and, as discussed, it represents the independent blade controllers as a controller on the collective flap action. Nevertheless, a verification of the resulting controller gains with HAWC2 non-linear time marching simulations confirms the good performance of the flap controller.

The tuning procedure is repeated with linear models obtained at different operating wind speeds above rated (**Table 6**). At all wind speeds, the first pole becoming unstable corresponds to the second collective flapwise mode, and the gains and the frequency at which instability occur slightly increase with wind speed. The corresponding proportional and, in a lower fashion, derivative gains also increase. To account for the increase, a gain scheduling is introduced as a linear function of the mean pitch angle $\bar{\theta}$ (**Figure 10**); the scheduling parameters k_{KP} and k_{KD} are retrieved by linear least-square fitting of the proportional and derivative gains found with the Ziegler-Nichols tuning (**Eq. 3**).

$$k_P = k_P^{ref} + k_{KP} \cdot (\bar{\theta} - \theta^{ref})$$
$$k_D = k_D^{ref} + k_{KD} \cdot (\bar{\theta} - \theta^{ref}) \quad \textbf{(Eq. 3)}$$
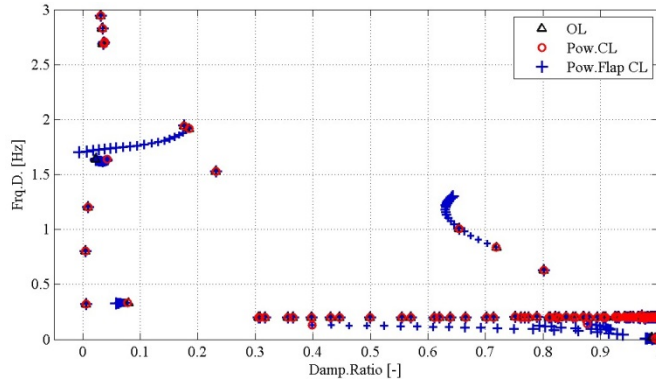
Figure 9 - Poles of the open and closed system for operation at 16m/s.

Table 6 – Overview of flap tuning parameters.

$\omega_c(M_x\ HPF)$	0.05 [Hz]
θ^{ref}	6.60x10^{-02}
k_P^{ref}, k_D^{ref}	3.75x10^{-03} [deg/kNm] 2.77x10^{-04} [deg/kNm]
k_{KP}, k_{KD}	1.94x10^{-03} [1/rad] 1.10x10^{-04} [1/rad]
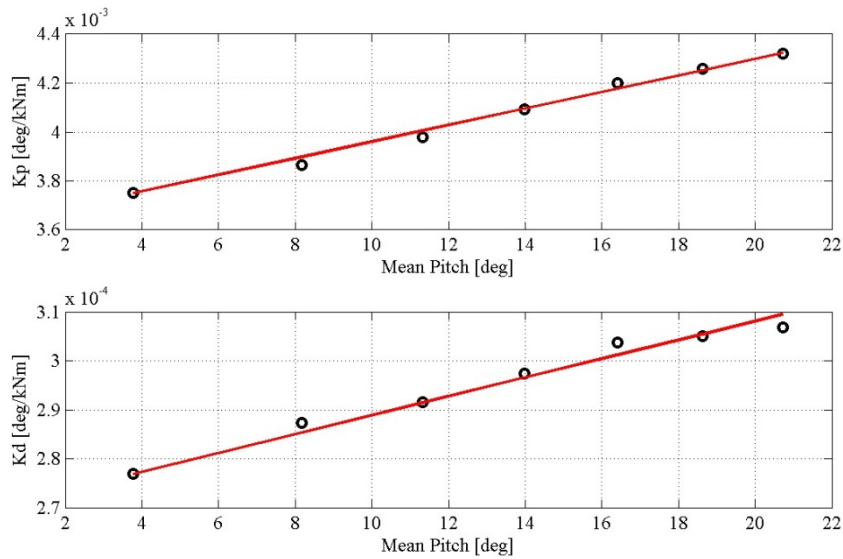
Figure 10 - Gain scheduling of the P and flap controller gains, based on the collective pitch angle.

Combined individual pitch and flap controller

In the case of the combined controller, the flap controller is added on top of the individual pitch controller. The individual pitch controller operates on the rotor level (tilt and yaw moments) and the flap controllers operate on each blade independently. The two controllers are implicitly separated by increasing the cut-off frequency of the high-pass filter on the flap control from 0.05Hz to 0.1Hz, thus forcing the flaps to react at higher frequencies, and thus avoid interaction

with the individual pitch system. The top level schematic of the combined controller is shown in **Figure 11**.

Figure 11 - Combined individual pitch and flap controller.

5. Results

In this section the results of the aeroelastic simulations on the full DLB are presented, and the different control concepts are compared.

Introduction

The results of all cases are analysed according to the post-processing procedure [**8**] and compared. The loads from normal operation DLC 1.2 are extrapolated to 50 year return loads, using the procedure by Natarajan and Holley [**10**]. The following configurations are considered and compared:

- Baseline
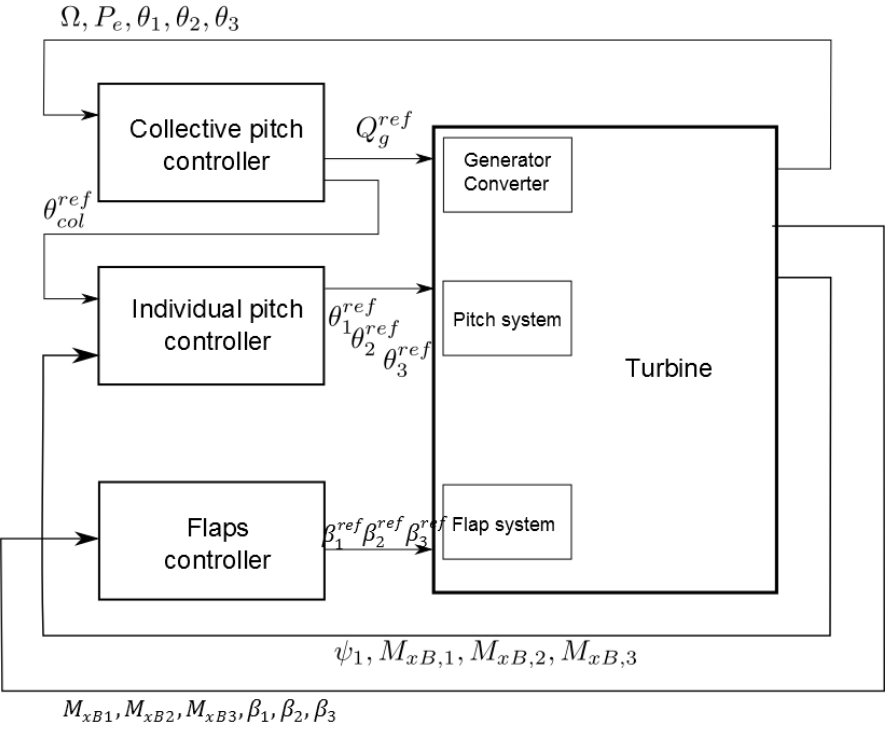- Individual pitch control
- Flap control
- Combined individual pitch and flap controls

The analysis is focusing on comparison of overall extreme (including partial safety factors (psf)) and lifetime fatigue loads from the full DLB, as well as comparison of short-term statistics of load and actuator activity channels. The load channels of interest and their associated parameters are shown in **Table 3**.

Baseline control

The baseline case data is found in [**19**]. The overall extreme loads are shown in **Table 7**, and lifetime fatigue loads in **Table 8 (**sensor names explaned in **Table 3)**. The loads resulting from extrapolation of DLC 1.1 are compared to the ones from DLC 1.3 and the overall extremes (incl. psf) in **Table 9**. An example of the resulting extrapolated load based on the DLC 1.1 data for the minimum flapwise root moment is shown in **Figure 12**.

Table 7 – Extreme loads (incl. psf) for the baseline case.

Name	Min incl. psf	Max incl. psf	DLC min	DLC max
MxTB	-2.12E+05	1.85E+05	23_wsp14_wdir000_s1005_tgl40	22b_wsp26_wdir000_s3012
MyTB	-1.73E+05	1.97E+05	61_wsp50_wdir352_s9986	61_wsp50_wdir008_s9996
MxTT	-3.17E+04	3.18E+04	22b_wsp26_wdir000_s3012	22b_wsp26_wdir000_s9012
MyTT	-5.06E+03	1.01E+04	51_wsp14_wdir000_s8006	81_wsp18_wdir008_s2108
MzTT	-2.91E+04	3.69E+04	22b_wsp26_wdir000_s3012	22b_wsp26_wdir000_s4012
MxMB	-2.47E+04	3.63E+04	13_wsp26_wdir350_s4012	22b_wsp26_wdir000_s4012
MyMB	-2.24E+04	2.41E+04	11_extrapolation	13_wsp26_wdir350_s3012
MzMB	-1.00E+04	9.73E+03	13_wsp26_wdir350_s3012	51_wsp12_wdir000_s6005
MxBR	-2.57E+04	1.87E+04	61_wsp50_wdir008_s9996	61_wsp50_wdir008_s9992
MyBR	-1.25E+04	1.11E+04	22y_wsp12_wdir270_s1205	22y_wsp24_wdir285_s2211
MzBR	-5.69E+02	5.88E+02	22y_wsp22_wdir075_s6010	62_wsp50_wdir225_s9990
TTDist	7.77E-01	-	22b_wsp24_wdir000_s1111	-

Table 8- Fatigue loads for the baseline case.

Sensor	Life time equivalent load	m	neq
MxTB	6.028E+04	4	1E+07
MyTB	2.779E+04	4	1E+07
MxTT	1.331E+04	4	1E+07
MyTT	1.690E+03	4	1E+07
MzTT	1.405E+04	4	1E+07
MxMB	1.626E+04	4	1E+07
MyMB	1.632E+04	4	1E+07
MzMB	3.209E+03	4	1E+07
MxBR	1.238E+04	10	1E+07
MyBR	8.745E+03	10	1E+07
MzBR	2.279E+02	10	1E+07
PitchActiv	1.690E+08	1	3E+06
PitchBearing	4.563E+19	3	1E+00

Table 9- Extrapolated loads (DLC 1.1) compared with DLC 1.3 and overall extreme loads for the baseline case (highlighted values indicate extrapolated loads exciding DLC 1.3 loads and/or overall extreme loads).

|	DLC1.1	psf	load	DLC1.3	psf	load	all DLC
MxBRmax	1.07E+04	1.25	1.33E+04	1.27E+04	1.35	1.71E+04	1.87E+04
MxBRmin	-1.60E+04	1.27	-2.03E+04	-1.63E+04	1.35	-2.21E+04	-2.57E+04
MxMBmax	1.72E+04	1.3	2.24E+04	1.81E+04	1.35	2.44E+04	3.63E+04
MxMBmin	-1.72E+04	1.27	-2.18E+04	-1.83E+04	1.35	-2.47E+04	-2.47E+04
MxTBmax	8.58E+04	1.25	1.07E+05	9.44E+04	1.35	1.27E+05	1.85E+05
MxTBmin	-2.91E+04	1.35	-3.93E+04	-6.34E+04	1.35	-8.56E+04	-2.12E+05
MxTTmax	1.70E+04	1.15	1.95E+04	1.92E+04	1.35	2.59E+04	3.18E+04
MxTTmin	-1.45E+04	1.22	-1.77E+04	-1.64E+04	1.35	-2.21E+04	-3.17E+04
MyBRmax	7.67E+03	1.12	8.59E+03	8.01E+03	1.35	1.08E+04	1.11E+04
MyBRmin	-6.86E+03	1.12	-7.69E+03	-7.29E+03	1.35	-9.84E+03	-1.25E+04
MyMBmax	1.67E+04	1.2	2.00E+04	1.79E+04	1.35	2.41E+04	2.41E+04
MyMBmin	-1.58E+04	1.42	**-2.24E+04**	-1.58E+04	1.35	-2.14E+04	**-2.14E+04**
MyTBmax	4.49E+04	1.11	4.99E+04	5.12E+04	1.35	6.91E+04	1.97E+05
MyTBmin	-3.43E+04	1.37	-4.70E+04	-3.81E+04	1.35	-5.15E+04	-1.73E+05
MyTTmax	6.08E+03	1.07	6.51E+03	6.15E+03	1.35	8.31E+03	1.01E+04
MyTTmin	-243.2106	1.21	-2.94E+02	-764.04	1.35	-1.03E+03	-5.06E+03
MzBRmax	215.43	1.42	3.06E+02	235.78	1.35	3.18E+02	5.88E+02
MzBRmin	-275.85	1.22	-3.37E+02	-266.94	1.35	-3.60E+02	-5.69E+02
MzMBmax	42.90	1.17	5.02E+01	554.19	1.35	7.48E+02	9.73E+03
MzMBmin	-6.92E+03	1.05	-7.26E+03	-7.41E+03	1.35	-1.00E+04	-1.00E+04
MzTTmax	2.03E+04	1.25	2.54E+04	1.98E+04	1.35	2.68E+04	3.69E+04
MzTTmin	-1.83E+04	1.37	**-2.50E+04**	-1.73E+04	1.35	-2.34E+04	-2.91E+04
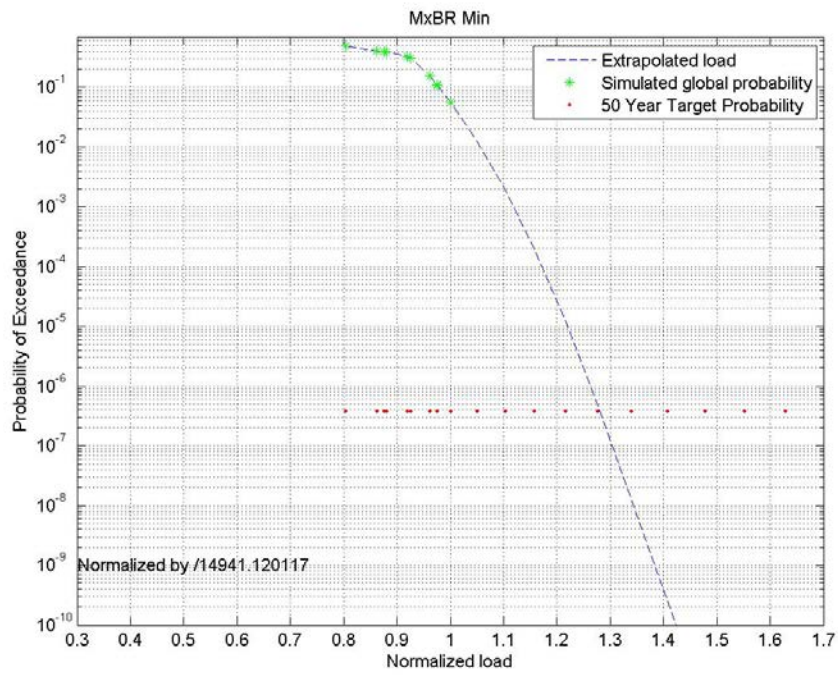
Figure 12 - Extrapolated value for the minimum flapwise root moment for the baseline case.

Individual pitch control

The baseline case data is found in [**20**]. The overall extreme loads are shown in **Table 10**, and lifetime fatigue loads in **Table 11**. The loads resulting from extrapolation of DLC 1.1 are compared to the ones from DLC 1.3 and the overall extremes (incl. psf) in **Table 12**. An example of the resulting extrapolated load based on the DLC 1.1 data for the minimum flapwise root moment is shown in **Figure 13**. Indicative comparison time series for the flapwise root moment and hub roll moment responses in DLC 1.2 are shown in **Figure 14** and **Figure 15** respectively and for the tower-tip distance in DLC 1.3 in **Figure 16**.

Table 10- Extreme loads (incl. psf) for the individual pitch control case.

Name	Min incl. psf	Max incl. psf	DLC min	DLC max
MxTB	-2.09E+05	1.95E+05	22y_wsp26_wdir300_s3212	22b_wsp26_wdir000_s3012
MyTB	-1.73E+05	1.97E+05	61_wsp50_wdir352_s9986	61_wsp50_wdir008_s9996
MxTT	-3.21E+04	3.14E+04	22y_wsp26_wdir300_s3212	22b_wsp26_wdir000_s7012
MyTT	-6.08E+03	1.01E+04	51_wsp14_wdir000_s1006	81_wsp18_wdir008_s2108
MzTT	-2.86E+04	3.82E+04	22b_wsp26_wdir000_s2012	22b_wsp26_wdir000_s4012
MxMB	-3.13E+04	3.77E+04	22y_wsp26_wdir300_s3212	22b_wsp26_wdir000_s4012
MyMB	-2.47E+04	2.62E+04	14_wsp14_wdir000_s0000	24_wsp26_wdir020_s4012
MzMB	-1.03E+04	9.86E+03	13_wsp26_wdir350_s3012	51_wsp12_wdir000_s6005
MxBR	-2.76E+04	2.17E+04	22y_wsp26_wdir300_s3212	22y_wsp26_wdir300_s3212
MyBR	-1.25E+04	1.08E+04	22y_wsp12_wdir270_s1205	13_wsp26_wdir000_s1012
MzBR	-5.08E+02	5.88E+02	62_wsp50_wdir225_s9990	62_wsp50_wdir225_s9990
TTDist	7.82E-01	-	22b_wsp24_wdir000_s1111	-

Table 11- Fatigue loads for the individual pitch control case.

Sensor	Life time equivalent load	m	neq
MxTB	6.078E+04	4	1E+07
MyTB	2.927E+04	4	1E+07
MxTT	1.288E+04	4	1E+07
MyTT	1.668E+03	4	1E+07
MzTT	1.344E+04	4	1E+07
MxMB	1.585E+04	4	1E+07
MyMB	1.593E+04	4	1E+07
MzMB	3.206E+03	4	1E+07
MxBR	1.023E+04	10	1E+07
MyBR	8.567E+03	10	1E+07
MzBR	2.287E+02	10	1E+07
PitchActiv	1.027E+09	1	3E+06
PitchBearing	1.055E+20	3	1E+00

Table 12- Extrapolated loads (DLC 1.1) compared with DLC 1.3 and overall extreme loads for the individual pitch control case (highlighted values indicate extrapolated loads exciding DLC 1.3 loads and/or overall extreme loads).

|	DLC1.1	psf	load	DLC1.3	psf	load	all DLC
MxBRmax	1.47E+04	1.25	1.84E+04	1.46E+04	1.35	1.97E+04	2.17E+04
MxBRmin	-1.59E+04	1.35	-2.15E+04	-1.63E+04	1.35	-2.21E+04	-2.76E+04
MxMBmax	1.60E+04	1.27	2.03E+04	1.90E+04	1.35	2.56E+04	3.77E+04
MxMBmin	-1.53E+04	1.38	-2.11E+04	1.90E+04	1.35	2.56E+04	-3.13E+04
MxTBmax	1.04E+05	1.45	**1.51E+05**	1.90E+04	1.35	2.56E+04	1.95E+05
MxTBmin	-1.02E+05	1.60	**-1.64E+05**	-1.66E+04	1.35	-2.24E+04	-2.09E+05
MxTTmax	1.60E+04	1.43	2.29E+04	1.99E+04	1.35	2.69E+04	3.14E+04
MxTTmin	-1.43E+04	1.19	-1.70E+04	-1.59E+04	1.35	-2.15E+04	-3.21E+04
MyBRmax	7.51E+03	1.19	8.93E+03	8.01E+03	1.35	1.08E+04	1.08E+04
MyBRmin	-6.46E+03	1.18	-7.62E+03	-7.27E+03	1.35	-9.81E+03	-1.25E+04
MyMBmax	1.71E+04	1.32	2.26E+04	1.90E+04	1.35	2.57E+04	2.62E+04
MyMBmin	-1.37E+04	1.34	-1.84E+04	-1.58E+04	1.35	-2.13E+04	-2.47E+04
MyTBmax	9.49E+04	1.25	**1.19E+05**	5.01E+04	1.35	6.76E+04	1.97E+05
MyTBmin	-6.57E+04	1.26	-8.28E+04	-4.21E+04	1.35	-5.68E+04	-1.73E+05
MyTTmax	5.71E+03	1.11	6.34E+03	5.89E+03	1.35	7.96E+03	1.01E+04
MyTTmin	-550.15	1.17	-6.44E+02	-649.24	1.35	-8.76E+02	-6.08E+03
MzBRmax	307.22	1.36	**4.18E+02**	3.09E+02	1.35	4.17E+02	5.88E+02
MzBRmin	-263.84	1.26	-3.32E+02	-274.73	1.35	-3.71E+02	-5.08E+02
MzMBmax	1.01E+03	1.18	1.19E+03	800.47	1.35	1.08E+03	9.86E+03
MzMBmin	-7.09E+03	1.05	-7.45E+03	-7.63E+03	1.35	-1.03E+04	-1.03E+04
MzTTmax	1.74E+04	1.62	**2.81E+04**	2.04E+04	1.35	2.76E+04	3.82E+04
MzTTmin	-1.21E+04	1.50	-1.81E+04	-1.39E+04	1.35	-1.87E+04	-2.86E+04
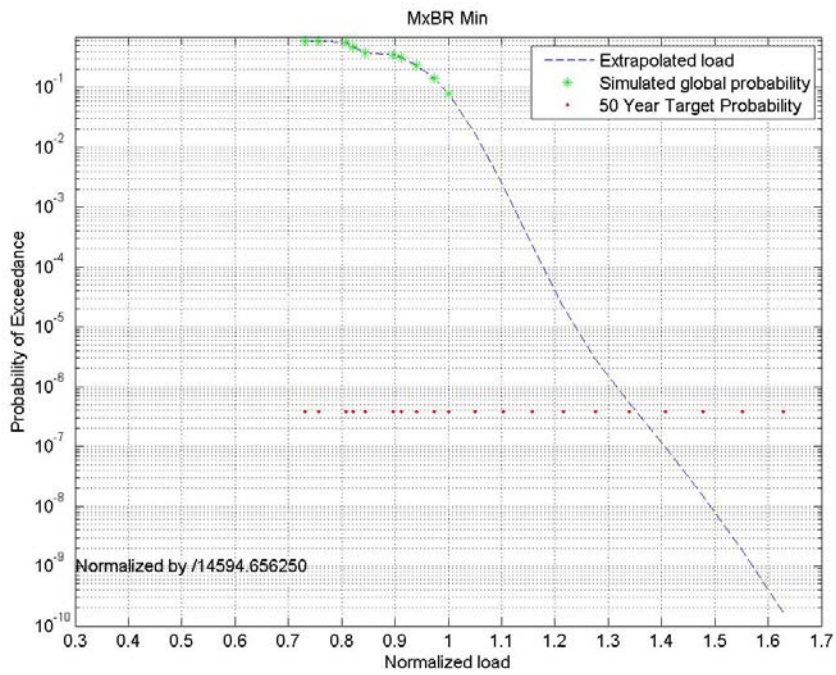
Figure 13- Extrapolated value for the minimum flapwise root moment for the individual pitch control case.
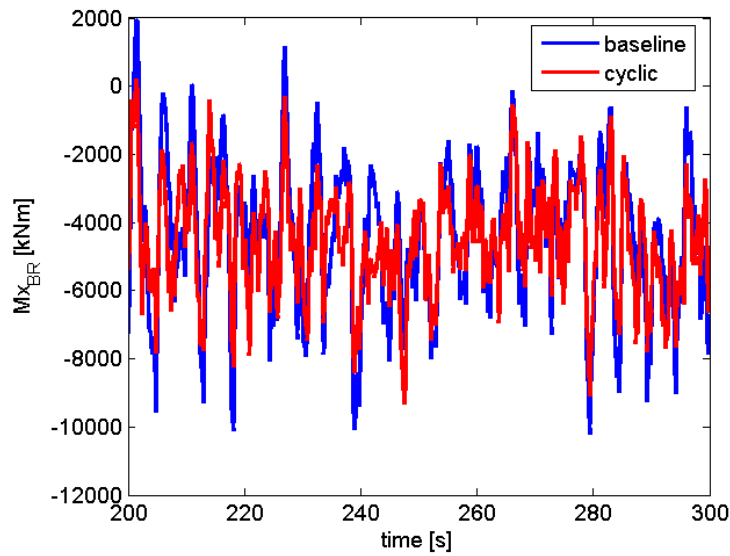

Figure 14 – Comparison of flapwise root moment response in DLC 1.2 at 16m/s: Baseline vs individual pitch control.
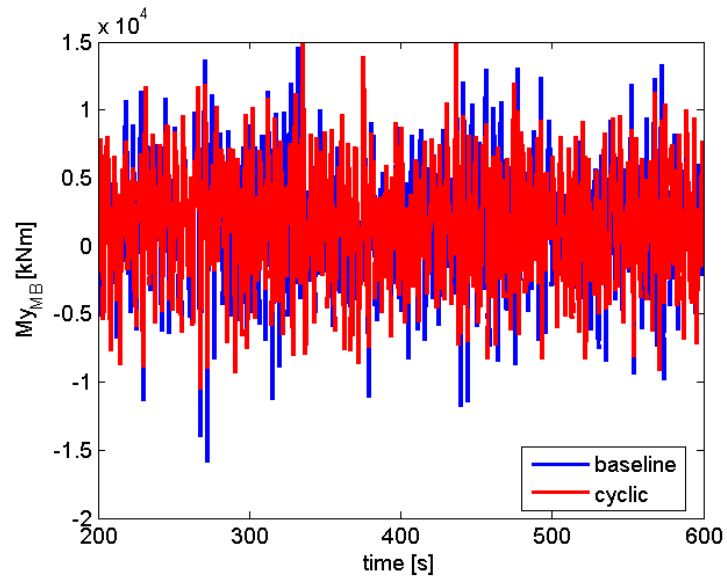
Figure 15 – Comparison of main bearing roll moment response in DLC 1.2 at 16m/s: Baseline vs individual pitch control.
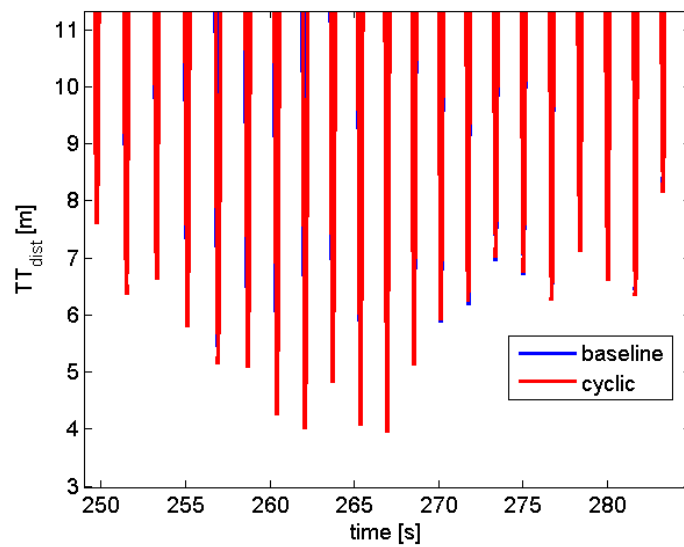

Figure 16 – Comparison of tip-tower distance in DLC 1.3 at 10m/s: Baseline vs individual pitch control.

Flap control

The baseline case data is found in [**21**]. The overall extreme loads are shown in **Table 13**, and lifetime fatigue loads in **Table 14**. The loads resulting from extrapolation of DLC 1.1 are compared to the ones from DLC 1.3 and the overall extremes (incl. psf) in **Table 15**. An example of the resulting extrapolated load based on the DLC 1.1 data for the minimum flapwise root moment is shown in **Figure 17**. Indicative comparison time series for the flapwise root moment and hub roll moment responses in DLC 1.2 are shown in **Figure 18** and **Figure 19** respectively and for the tower-tip distance in DLC 1.3 in **Figure 20**.

Table 13 – Extreme loads (incl. psf) for the flap controls case.

Name	Min incl. psf	Max incl. psf	DLC min	DLC max
MxTB	-2.11E+05	1.76E+05	23_wsp14_wdir000_s1005_tgl40	22b_wsp26_wdir000_s8012
MyTB	-1.73E+05	1.97E+05	61_wsp50_wdir352_s9986	61_wsp50_wdir008_s9996
MxTT	-3.21E+04	3.43E+04	22b_wsp26_wdir000_s6012	22b_wsp26_wdir000_s3112
MyTT	-5.08E+03	1.01E+04	51_wsp14_wdir000_s8006	81_wsp18_wdir008_s2108
MzTT	-3.25E+04	3.82E+04	22b_wsp26_wdir000_s7012	22b_wsp26_wdir000_s7012
MxMB	-2.15E+04	3.88E+04	13_wsp24_wdir010_s6011	22b_wsp26_wdir000_s7012
MyMB	-1.90E+04	2.36E+04	13_wsp22_wdir000_s1010	22f2_wsp18_wdir000_s7008
MzMB	-1.01E+04	9.39E+03	13_wsp24_wdir010_s6011	51_wsp12_wdir000_s6005
MxBR	-2.71E+04	1.87E+04	22b_wsp26_wdir000_s5012	61_wsp50_wdir008_s9992
MyBR	-1.25E+04	1.22E+04	22y_wsp12_wdir270_s1205	22b_wsp24_wdir000_s1111
MzBR	-6.34E+02	5.88E+02	22b_wsp26_wdir000_s7012	62_wsp50_wdir225_s9990
TTDist	7.44E-01	-	22b_wsp26_wdir000_s4012	-

Table 14– Fatigue loads for the flap controls case.

Sensor	Life time equivalent load	m	neq
MxTB	5.912E+04	4	1E+07
MyTB	2.666E+04	4	1E+07
MxTT	1.299E+04	4	1E+07
MyTT	1.669E+03	4	1E+07
MzTT	1.373E+04	4	1E+07
MxMB	1.473E+04	4	1E+07
MyMB	1.479E+04	4	1E+07
MzMB	3.232E+03	4	1E+07
MxBR	1.057E+04	10	1E+07
MyBR	9.451E+03	10	1E+07
MzBR	2.502E+02	10	1E+07
FlapActiv	8.603E+09	1	3E+06
PitchActiv	2.122E+08	1	3E+06
PitchBearing	4.409E+19	3	1E+00

15 - Extrapolated loads (DLC 1.1) compared with DLC 1.3 and overall extreme loads for the flap controls case (highlighted values indicate extrapolated loads exciding DLC 1.3 loads and/or overall extreme loads).

|	DLC1.1	psf	load	DLC1.3	psf	load	all DLC
MxBRmax	9.33E+03	1.25	1.17E+04	1.14E+04	1.35	1.53E+04	1.87E+04
MxBRmin	-1.46E+04	1.30	-1.90E+04	-1.63E+04	1.35	-2.20E+04	-2.71E+04
MxMBmax	1.46E+04	1.42	**2.07E+04**	1.51E+04	1.35	2.04E+04	3.88E+04
MxMBmin	-1.56E+04	1.25	-1.95E+04	-1.59E+04	1.35	-2.15E+04	-2.15E+04
MxTBmax	8.12E+04	1.14	9.26E+04	9.00E+04	1.35	1.22E+05	1.76E+05
MxTBmin	-2.91E+04	1.35	-3.93E+04	-6.34E+04	1.35	-8.56E+04	-2.11E+05
MxTTmax	1.49E+04	1.34	1.99E+04	1.67E+04	1.35	2.25E+04	1.76E+05
MxTTmin	-1.24E+04	1.29	-1.60E+04	-1.39E+04	1.35	-1.87E+04	-3.21E+04
MyBRmax	8.62E+03	1.20	1.03E+04	8.52E+03	1.35	1.15E+04	1.22E+04
MyBRmin	-7.22E+03	1.25	-9.02E+03	-7.96E+03	1.35	-1.07E+04	-1.25E+04
MyMBmax	1.48E+04	1.34	1.99E+04	1.54E+04	1.35	2.08E+04	2.36E+04
MyMBmin	-1.33E+04	1.26	-1.67E+04	-1.41E+04	1.35	-1.90E+04	-1.90E+04
MyTBmax	4.06E+04	1.13	4.59E+04	4.99E+04	1.35	6.73E+04	1.97E+05
MyTBmin	-3.18E+04	1.38	-4.39E+04	-3.52E+04	1.35	-4.75E+04	-1.73E+05
MyTTmax	5.91E+03	1.13	6.68E+03	5.99E+03	1.35	8.09E+03	1.01E+04
MyTTmin	-243.21	1.17	-2.85E+02	-764.04	1.35	-1.03E+03	-5.08E+03
MzBRmax	213.97	1.25	2.67E+02	2.35E+02	1.35	3.18E+02	1.22E+04
MzBRmin	-282.53	1.27	-3.59E+02	-2.75E+02	1.35	-3.72E+02	-1.25E+04
MzMBmax	4.29E+01	1.11	4.76E+01	554.19	1.35	7.48E+02	9.39E+03
MzMBmin	-7.12E+03	1.10	-7.83E+03	-7.47E+03	1.35	-1.01E+04	-1.01E+04
MzTTmax	1.88E+04	1.24	**2.33E+04**	1.71E+04	1.35	2.31E+04	3.82E+04
MzTTmin	-1.55E+04	1.20	-1.86E+04	-1.53E+04	1.35	-2.06E+04	-3.25E+04
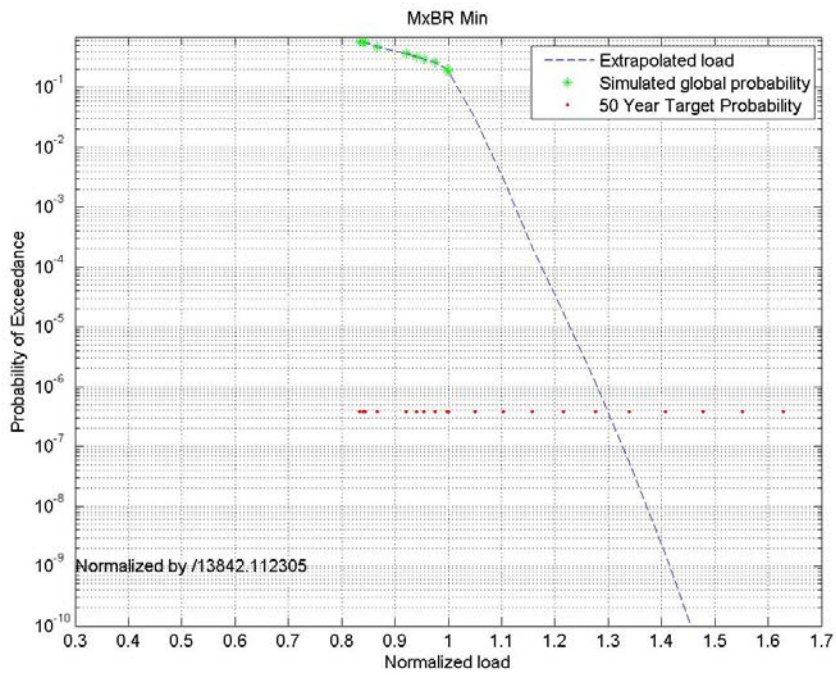
Figure 17- Extrapolated value for the minimum flapwise root moment for the flap controls case.
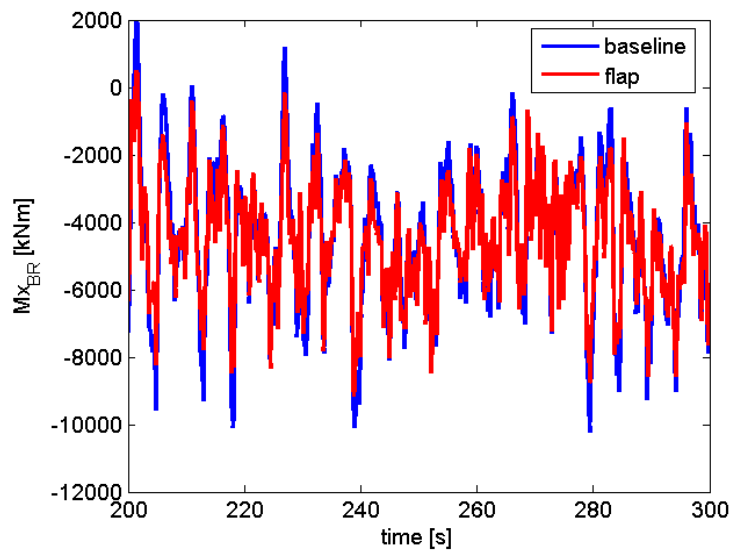

Figure 18– Comparison of flapwise root moment response in DLC 1.2 at 16m/s: Baseline vs flap controls.
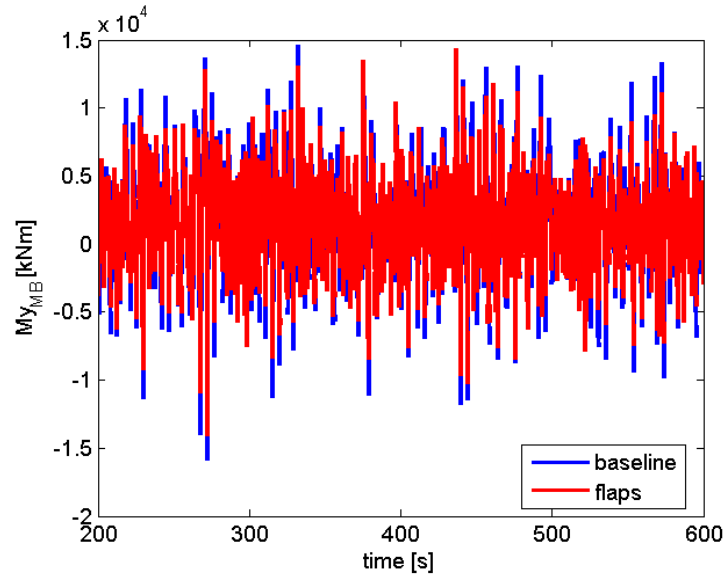
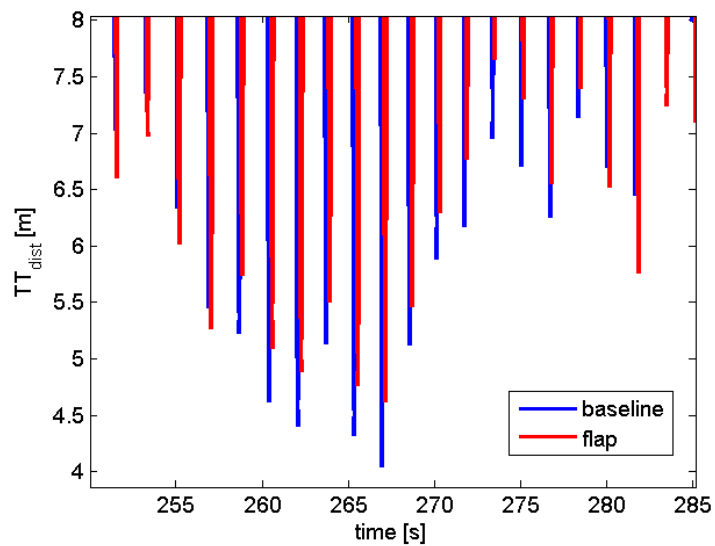**Figure 19– Comparison of main bearing roll moment response in DLC 1.2 at 16m/s: Baseline vs flap controls.**

Figure 20 - Comparison of tip-tower distance in DLC 1.3 at 10m/s: Baseline vs flaps control.

Combined individual pitch and flap controls

The baseline case data is found in [**22**]. The overall extreme loads are shown in **Table 16**, and lifetime fatigue loads in **Table 17**. The loads resulting from extrapolation of DLC 1.1 are compared to the ones from DLC 1.3 and the overall extremes (incl. psf) in **Table 18**. An example of the resulting extrapolated load based on the DLC 1.1 data for the minimum flapwise root moment is shown in **Figure 21**. Indicative comparison time series for the flapwise root moment and hub roll moment responses in DLC 1.2 are shown in **Figure 22** and **Figure 23** respectively and for the tower-tip distance in DLC 1.3 in **Figure 24**.

Table 16 - Extreme loads (incl. psf) for the combined individual pitch and flap controls case.

Name	Min incl. psf	Max incl. psf	DLC min	DLC max
MxTB	-2.05E+05	1.83E+05	51_wsp12_wdir000_s4005	22b_wsp26_wdir000_s8012
MyTB	-1.73E+05	1.97E+05	61_wsp50_wdir352_s9986	61_wsp50_wdir008_s9996
MxTT	-3.50E+04	3.32E+04	22b_wsp26_wdir000_s9012	22b_wsp26_wdir000_s3012
MyTT	-5.47E+03	1.01E+04	51_wsp14_wdir000_s1006	81_wsp18_wdir008_s2108
MzTT	-3.32E+04	3.47E+04	22b_wsp26_wdir000_s4012	22b_wsp26_wdir000_s4012
MxMB	-1.93E+04	3.78E+04	13_wsp26_wdir350_s4012	22b_wsp26_wdir000_s6012
MyMB	-1.83E+04	2.18E+04	11_extrapolation	21_wsp26_wdir350_s6012
MzMB	-1.03E+04	9.59E+03	13_wsp26_wdir350_s3012	51_wsp12_wdir000_s6005
MxBR	-2.75E+04	1.87E+04	22b_wsp26_wdir000_s5012	61_wsp50_wdir008_s9992
MyBR	-1.25E+04	1.20E+04	22y_wsp12_wdir270_s1205	22b_wsp26_wdir000_s4012
MzBR	-6.02E+02	5.88E+02	22y_wsp26_wdir075_s6012	62_wsp50_wdir225_s9990
TTDist	7.09E-01	-	22b_wsp26_wdir000_s7012	-

Table 17 - Extreme loads (incl. psf) for the combined individual pitch and flap controls case.

Sensor	Life time equivalent load	m	neq
MxTB	5.922E+04	4	1E+07
MyTB	2.704E+04	4	1E+07
MxTT	1.283E+04	4	1E+07
MyTT	1.650E+03	4	1E+07
MzTT	1.333E+04	4	1E+07
MxMB	1.507E+04	4	1E+07
MyMB	1.518E+04	4	1E+07
MzMB	3.234E+03	4	1E+07
MxBR	9.234E+03	10	1E+07
MyBR	9.329E+03	10	1E+07
MzBR	2.413E+02	10	1E+07
FlapActiv	8.647E+09	1	3E+06
PitchActiv	8.299E+08	1	3E+06
PitchBearing	9.247E+19	3	1E+00

Table 18 - Extrapolated loads (DLC 1.1) compared with DLC 1.3 and overall extreme loads for the combined individual pitch and flap controls case (highlighted values indicate extrapolated loads exciding DLC 1.3 loads and/or overall extreme loads).

|	DLC1.1	psf	load	DLC1.3	psf	load	all DLC
MxBRmax	7.43E+03	1.25	9.29E+03	1.01E+04	1.35	1.36E+04	1.87E+04
MxBRmin	-1.46E+04	1.35	-1.97E+04	-1.63E+04	1.35	-2.20E+04	-2.75E+04
MxMBmax	1.34E+04	1.16	1.56E+04	1.45E+04	1.35	1.95E+04	3.78E+04
MxMBmin	-1.30E+04	1.37	-1.78E+04	-1.43E+04	1.35	-1.93E+04	-1.93E+04
MxTBmax	8.02E+04	1.30	1.04E+05	8.92E+04	1.35	1.20E+05	1.83E+05
MxTBmin	-4.63E+04	1.20	-5.56E+04	-6.34E+04	1.35	-8.56E+04	-2.05E+05
MxTTmax	1.20E+04	1.30	1.56E+04	1.42E+04	1.35	1.92E+04	3.32E+04
MxTTmin	-1.24E+04	1.26	-1.57E+04	-1.39E+04	1.35	-1.88E+04	1.01E+04
MyBRmax	8.51E+03	1.24	1.06E+04	8.17E+03	1.35	1.10E+04	1.20E+04
MyBRmin	-7.11E+03	1.24	-8.82E+03	-7.62E+03	1.35	-1.03E+04	-1.25E+04
MyMBmax	1.37E+04	1.40	1.91E+04	1.60E+04	1.35	2.16E+04	2.18E+04
MyMBmin	-1.22E+04	1.50	**-1.83E+04**	-1.31E+04	1.35	-1.77E+04	**-1.77E+04**
MyTBmax	4.42E+04	1.40	6.18E+04	4.73E+04	1.35	6.38E+04	1.83E+05
MyTBmin	-3.37E+04	1.51	**-5.09E+04**	-3.57E+04	1.35	-4.82E+04	-2.05E+05
MyTTmax	5.74E+03	1.06	6.09E+03	5.82E+03	1.35	7.86E+03	3.32E+04
MyTTmin	-497.75	1.13	-5.62E+02	-649.24	1.35	-8.76E+02	-3.50E+04
MzBRmax	215.20	1.41	3.03E+02	2.48E+02	1.35	3.35E+02	5.88E+02
MzBRmin	-272.04	1.25	-3.40E+02	-2.66E+02	1.35	-3.59E+02	-6.02E+02
MzMBmax	5.16E+02	1.25	6.46E+02	592.20	1.35	7.99E+02	9.59E+03
MzMBmin	-7.25E+03	1.10	-7.98E+03	-7.61E+03	1.35	-1.03E+04	-1.03E+04
MzTTmax	1.58E+04	1.26	1.99E+04	1.58E+04	1.35	2.13E+04	3.47E+04
MzTTmin	-1.21E+04	1.41	-1.71E+04	-1.36E+04	1.35	-1.84E+04	-3.32E+04
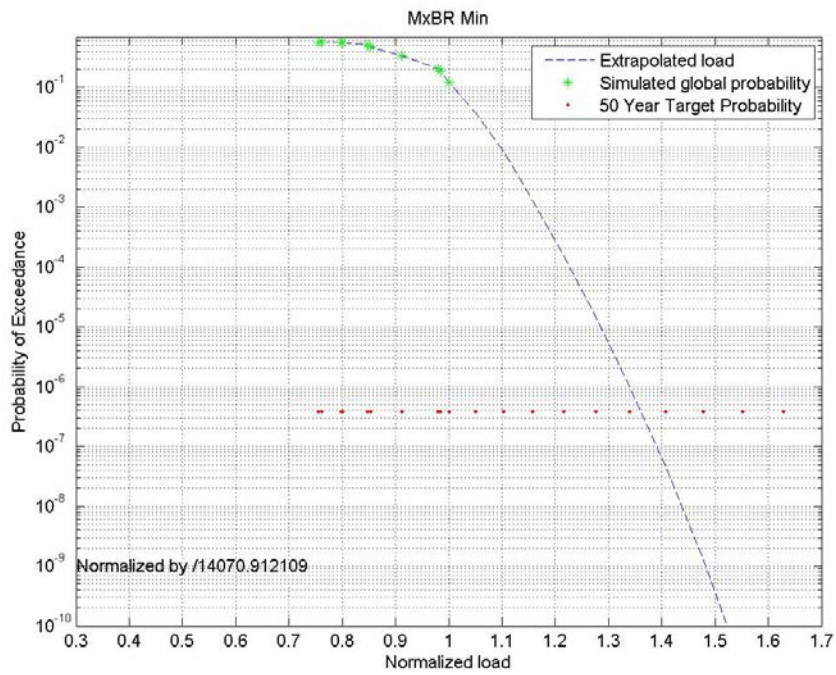
Figure 21- Extrapolated value for the minimum flapwise root moment for the combined individual pitch and flap controls case.
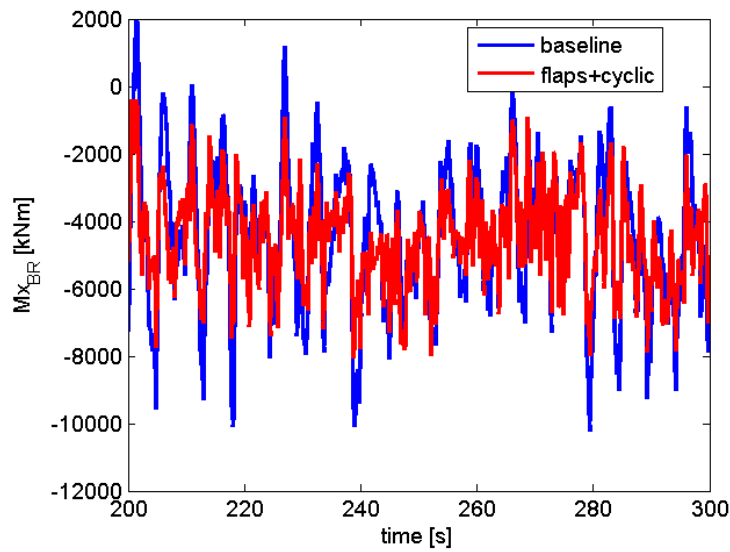

Figure 22– Comparison of flapwise root moment response in DLC 1.2 at 16m/s: Baseline vs combined individual pitch and flap controls.
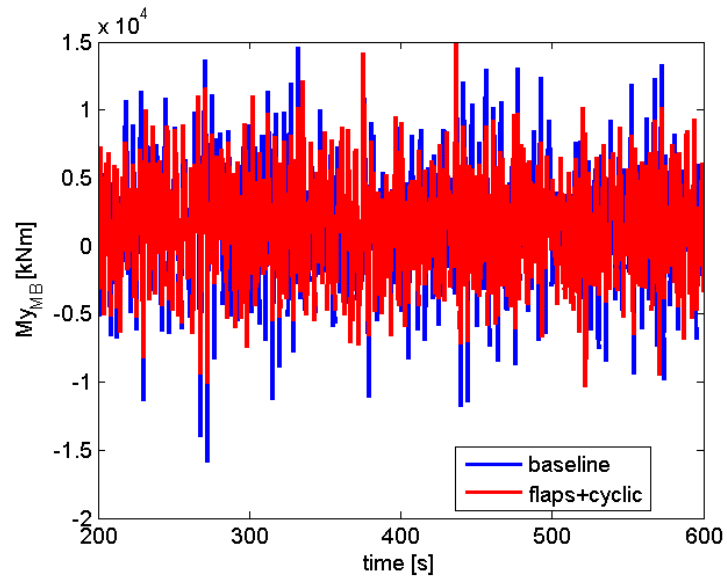
Figure 23– Comparison of main bearing roll moment response in DLC 1.2 at 16m/s: Baseline vs combined individual pitch and flap controls.
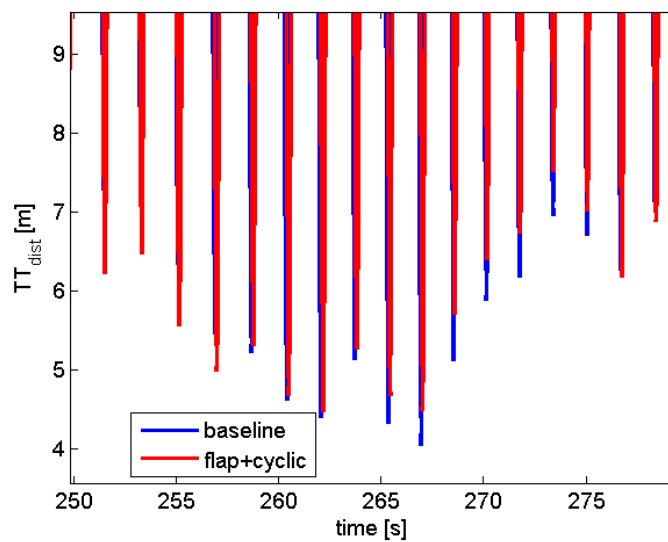

Figure 24– Comparison of tip-tower distance in DLC 1.3 at 10m/s: Baseline vs combined individual pitch and flap controls.

Comparison of cases

The overall extreme loads for all cases are compared in terms of the overall extreme maximum (**Figure 25**), extreme minimum (**Figure 26**), and lifetime fatigue (**Figure 27**) values. The comparison for all values is shown in **Table 19**, where also the lifetime pitch bearing damage and pitch and flap activities are included.
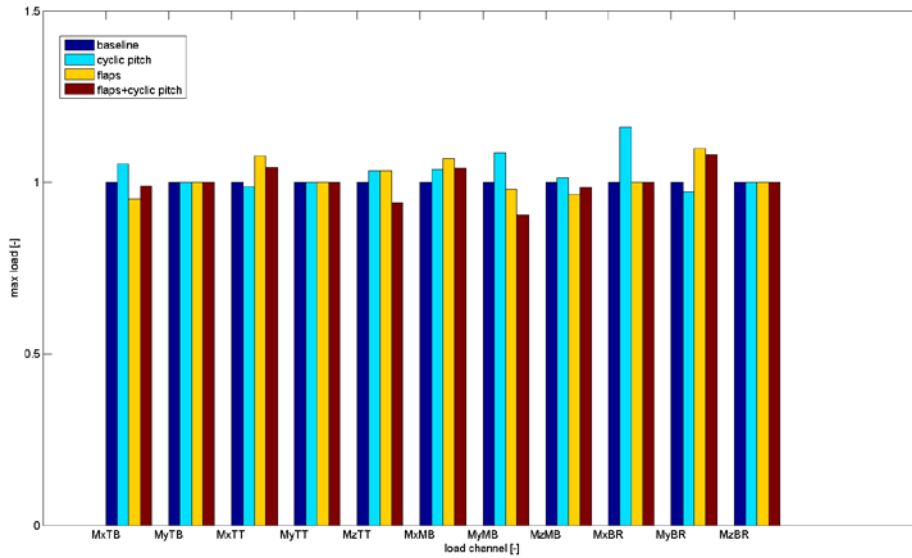

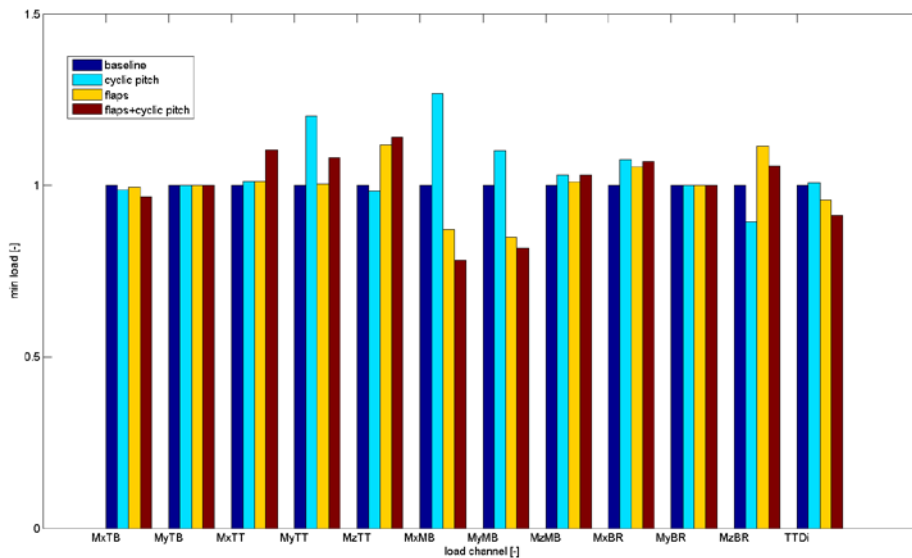**Figure 25 – Comparison of extreme maximum loads between cases (loads normalized by baseline loads).**

Figure 26 - Comparison of extreme minimum loads between cases (loads normalized by baseline loads).
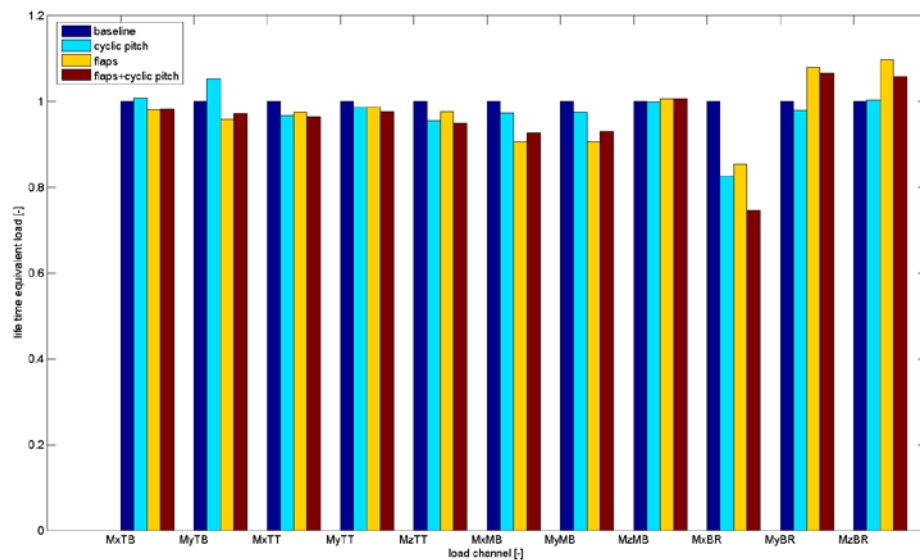
Figure 27 - Comparison of lifetime fatigue loads between cases (loads normalized by baseline loads).

All the three control concepts significantly reduce the lifetime fatigue loads for certain load channels, like the flapwise root moment (M_xBR), which is the load channel targeted by the load control algorithms. The load reduction is achieved at the cost of higher actuators activity: the pitch activity for the individual pitch configuration is ten times higher than the baseline one, but the pitch bearing equivalent damage [**9**] increases only by a factor of two, as the flapwise load variation is reduced. The flap control case present a slight increase of the pitch activity, thus indicating some interaction between the controllers; nevertheless the pitch equivalent damage is reduced (-3.4%), as the loads on the bearing are alleviated. The combination of both flap and individual pitch returns the highest fatigue load alleviation, and also allows to ease the demand on the pitch actuators, whose total travelled distance is 20 % lower than in the individual pitch control case.

As expected, the flap controls result in increased blade torsion loads due to the increased pitching moment. The impact on extreme loads is less clear, where on average flap and combined controls show increased or decreased loads in few channels and generally show no impact. The individual pitch controller results in increased loading in some channels and no impact on most of them.

The design load cases showing extreme loads are shown in **Table 19**, where it is seen that they are mostly connected in blade fault or parked cases. More detailed fine tuning of controller parameters on a case specific way could potentially eliminate some of these cases.

Table 19 - Comparison of extreme and fatigue loads for all cases (loads highlighted in yellow are extreme loads resulting from extrapolation)

EXTREME

	baseline C0032				cyclic C0037						flap C0034						combined C0035					
Name	Min	Max	DLC min	DLC max	Min	Max	DLC min	DLC max	% diff min	% diff max	Min	Max	DLC min	DLC max	% diff min	% diff max	Min	Max	DLC min	DLC max	% diff min	% diff max
MxTB	-2.12E+05	1.85E+05	23_wsp14_wdir000_s1005_tgl40	22b_wsp26_wdir000_s3012	-2.09E+05	1.95E+05	22y_wsp26_wdir300_s3212	22b_wsp26_wdir000_s3012	-1.42	5.41	-2.11E+05	1.76E+05	23_wsp14_wdir000_s1005_tgl40	22b_wsp26_wdir000_s8012	-0.47	-4.86	-2.05E+05	1.83E+05	51_wsp12_wdir000_s4005	22b_wsp26_wdir000_s8012	-3.30	-1.08
MyTB	-1.73E+05	1.97E+05	61_wsp50_wdir352_s9986	61_wsp50_wdir008_s9996	-1.73E+05	1.97E+05	61_wsp50_wdir352_s9986	61_wsp50_wdir008_s9996	0.00	0.00	-1.73E+05	1.97E+05	61_wsp50_wdir352_s9986	61_wsp50_wdir008_s9996	0.00	0.00	-1.73E+05	1.97E+05	61_wsp50_wdir352_s9986	61_wsp50_wdir008_s9996	0.00	0.00
MxTT	-3.17E+04	3.18E+04	22b_wsp26_wdir000_s3012	22b_wsp26_wdir000_s9012	-3.21E+04	3.14E+04	22y_wsp26_wdir300_s3212	22b_wsp26_wdir000_s7012	1.26	-1.26	-3.21E+04	3.43E+04	22b_wsp26_wdir000_s6012	22b_wsp26_wdir000_s3112	1.26	7.86	-3.50E+04	3.32E+04	22b_wsp26_wdir000_s9012	22b_wsp26_wdir000_s3012	10.41	4.40
MyTT	-5.06E+03	1.01E+04	51_wsp14_wdir000_s8006	81_wsp18_wdir008_s2108	-6.08E+03	1.01E+04	51_wsp14_wdir000_s1006	81_wsp18_wdir008_s2108	20.16	0.00	-5.08E+03	1.01E+04	51_wsp14_wdir000_s8006	81_wsp18_wdir008_s2108	0.40	0.00	-5.47E+03	1.01E+04	51_wsp14_wdir000_s1006	81_wsp18_wdir008_s2108	8.10	0.00
MzTT	-2.91E+04	3.69E+04	22b_wsp26_wdir000_s3012	22b_wsp26_wdir000_s4012	-2.86E+04	3.82E+04	22b_wsp26_wdir000_s2012	22b_wsp26_wdir000_s4012	-1.72	3.52	-3.25E+04	3.82E+04	22b_wsp26_wdir000_s7012	22b_wsp26_wdir000_s7012	11.68	3.52	-3.32E+04	3.47E+04	22b_wsp26_wdir000_s4012	22b_wsp26_wdir000_s4012	14.09	-5.96
MxMB	-2.47E+04	3.63E+04	13_wsp26_wdir350_s4012	22b_wsp26_wdir000_s4012	-3.13E+04	3.77E+04	22y_wsp26_wdir300_s3212	22b_wsp26_wdir000_s4012	26.72	3.86	-2.15E+04	3.88E+04	13_wsp24_wdir010_s6011	22b_wsp26_wdir000_s7012	-12.96	6.89	-1.93E+04	3.78E+04	13_wsp26_wdir350_s4012	22b_wsp26_wdir000_s6012	-21.86	4.13
MyMB	-2.24E+04	2.41E+04	13_wsp22_wdir000_s1010	11_extrapolation	-2.47E+04	2.62E+04	14_wsp14_wdir000_s0000	24_wsp26_wdir020_s4012	10.27	8.71	-1.90E+04	2.36E+04	13_wsp22_wdir000_s1010	22f2_wsp18_wdir000_s7008	-15.18	-2.07	-1.83E+04	2.18E+04	11_extrapolation	21_wsp26_wdir350_s6012	-18.30	-9.54
MzMB	-1.00E+04	9.73E+03	13_wsp26_wdir350_s3012	51_wsp12_wdir000_s6005	-1.03E+04	9.86E+03	13_wsp26_wdir350_s3012	51_wsp12_wdir000_s6005	3.00	1.34	-1.01E+04	9.39E+03	13_wsp24_wdir010_s6011	51_wsp12_wdir000_s6005	1.00	-3.49	-1.03E+04	9.59E+03	13_wsp26_wdir350_s3012	51_wsp12_wdir000_s6005	3.00	-1.44
MxBR	-2.57E+04	1.87E+04	61_wsp50_wdir008_s9996	61_wsp50_wdir008_s9992	-2.76E+04	2.17E+04	22y_wsp26_wdir300_s3212	22y_wsp26_wdir300_s3212	7.39	16.04	-2.71E+04	1.87E+04	22b_wsp26_wdir000_s5012	61_wsp50_wdir008_s9992	5.45	0.00	-2.75E+04	1.87E+04	22b_wsp26_wdir000_s5012	61_wsp50_wdir008_s9992	7.00	0.00
MyBR	-1.25E+04	1.11E+04	22y_wsp12_wdir270_s1205	22y_wsp24_wdir285_s2211	-1.25E+04	1.08E+04	22y_wsp12_wdir270_s1205	13_wsp26_wdir000_s1012	0.00	-2.70	-1.25E+04	1.22E+04	22y_wsp12_wdir270_s1205	22b_wsp26_wdir000_s1111	0.00	9.91	-1.25E+04	1.20E+04	22y_wsp12_wdir270_s1205	22b_wsp26_wdir000_s4012	0.00	8.11
MzBR	-5.69E+02	5.88E+02	22y_wsp22_wdir075_s6010	62_wsp50_wdir225_s9990	-5.08E+02	5.88E+02	62_wsp50_wdir225_s9990	62_wsp50_wdir225_s9990	-10.72	0.00	-6.34E+02	5.88E+02	22b_wsp26_wdir000_s7012	62_wsp50_wdir225_s9990	11.42	0.00	-6.02E+02	5.88E+02	22y_wsp12_wdir075_s6012	62_wsp50_wdir225_s9990	5.80	0.00
TTDist	7.77E-01	-	22b_wsp24_wdir000_s1111	-	7.82E-01	-	22b_wsp24_wdir000_s1111	-	0.64	-	7.44E-01	-	22b_wsp26_wdir000_s4012	-	-4.25	-	7.09E-01	-	22b_wsp26_wdir000_s7012	-	-8.75	-

FATIGUE

	C0032	cyclic C0037		flap C0034		combined C0035	
Name	LEqL	LEqL	% diff min	LEqL	% diff min	LEqL	% diff min
MxTB	6.03E+04	6.08E+04	0.83	5.91E+04	-1.92	5.92E+04	-1.76
MyTB	2.78E+04	2.93E+04	5.33	2.67E+04	-4.07	2.70E+04	-2.70
MxTT	1.33E+04	1.29E+04	-3.23	1.30E+04	-2.40	1.28E+04	-3.61
MyTT	1.69E+03	1.67E+03	-1.30	1.67E+03	-1.24	1.65E+03	-2.37
MzTT	1.41E+04	1.34E+04	-4.34	1.37E+04	-2.28	1.33E+04	-5.12
MxMB	1.63E+04	1.59E+04	-2.52	1.47E+04	-9.41	1.51E+04	-7.32
MyMB	1.63E+04	1.59E+04	-2.39	1.48E+04	-9.38	1.52E+04	-6.99
MzMB	3.21E+03	3.21E+03	-0.09	3.23E+03	0.72	3.23E+03	0.78
MxBR	1.24E+04	1.02E+04	-17.37	1.06E+04	-14.62	9.23E+03	-25.41
MyBR	8.75E+03	8.57E+03	-2.04	9.45E+03	8.07	9.33E+03	6.68
MzBR	2.28E+02	2.29E+02	0.35	2.50E+02	9.78	2.41E+02	5.88
Pitch activity	1.69E+08	1.03E+09	507.69	2.12E+08	25.56	8.30E+08	391.07
Flap activity	0.00E+00	0.00E+00	-	8.60E+09	100.00	8.65E+09	0.51
PitchBearing	4.56E+19	1.06E+20	131.21	4.41E+19	-3.37	9.25E+19	102.65

In **Figure 28**, the short term equivalent load statistics for the blade root flapwise moment in DLC 1.2 are shown for every wind speed, where all cases are compared. It is seen that on average the individual pitch and flap controls achieve considerable reduction of fatigue loading in full load operation, with increased alleviation when combined.
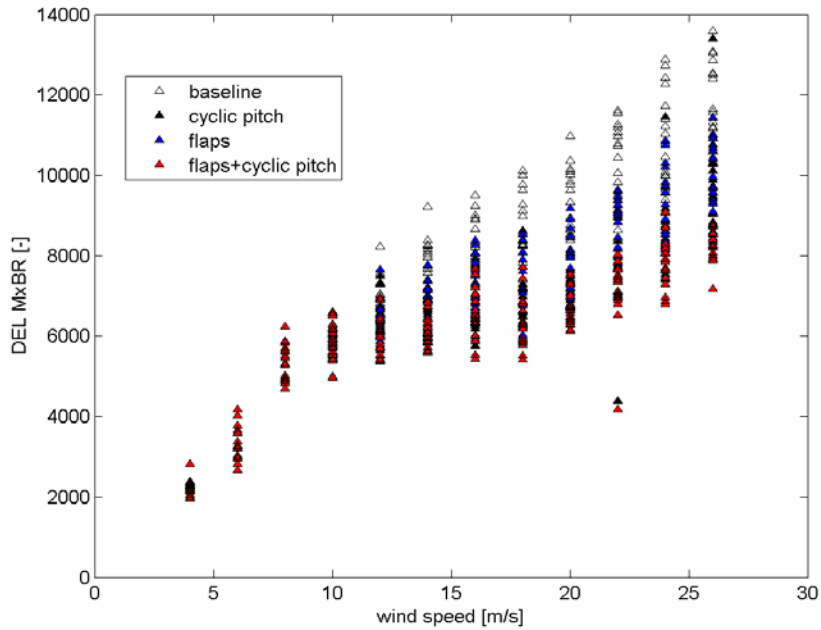

Figure 28 – Comparison of flapwise root moment short term fatigue equivalent loads between cases for DLC 1.2.

In **Figure 29**, the short term equivalent load statistics for the tower root fore-aft moment in DLC 1.2 are shown for every wind speed, where all cases are compared. It is seen that on average the flap controls and combined controls achieve considerable reduction of fatigue loading in full load operation, while the individual pitch control targeting at rotor imbalance loading shows a slight increase of loads.
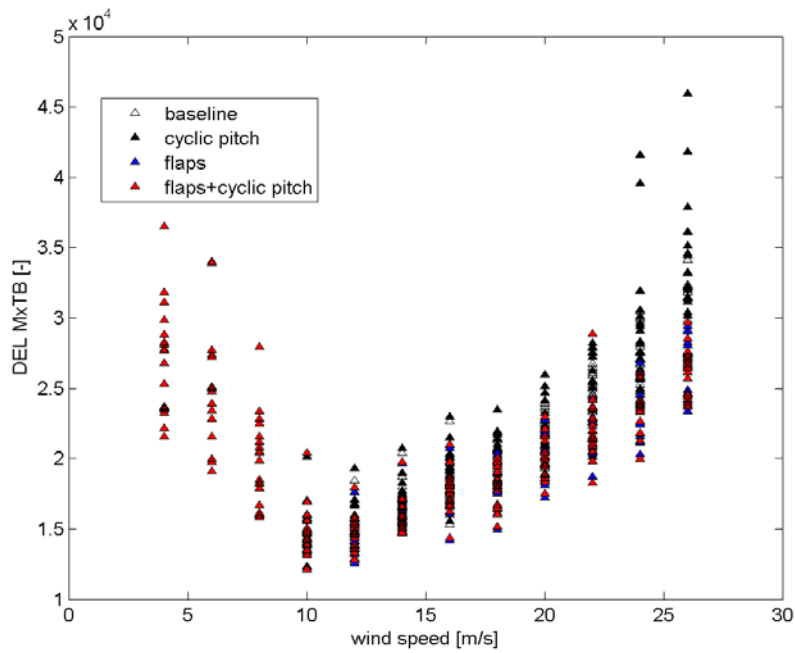
Figure 29 – Comparison of fore-aft tower root moment short term fatigue equivalent loads between cases for DLC 1.2.

In **Figure 30**, the minimum tower-tip distance in DLC 1.2 is shown for every wind speed, where all cases are compared. It is seen that on average the flap controls and combined controls achieve increase of the distance, while the individual pitch control shows a slight decrease.
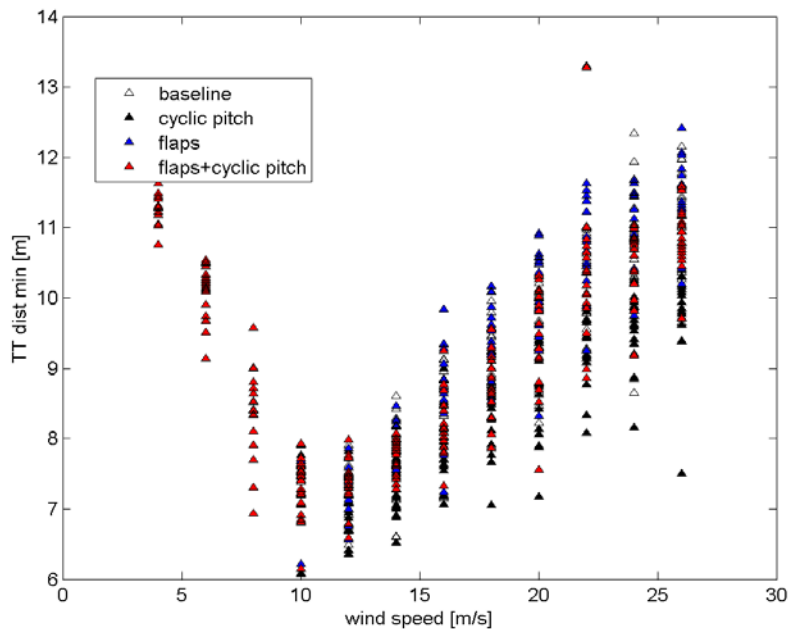

Figure 30 – Comparison of minimum tip-tower distance (no psf) between cases for DLC 1.2.

In **Figure 31**, the pitch bearing short term equivalent loads in DLC 1.2 are shown for every wind speed, where all cases are compared. It is seen that on average the individual pitch controls increase considerable the bearing damage, while the flap controls slightly decrease it (compared to the baseline) and the combined controls show a slight decrease compared to the individual pitch control.
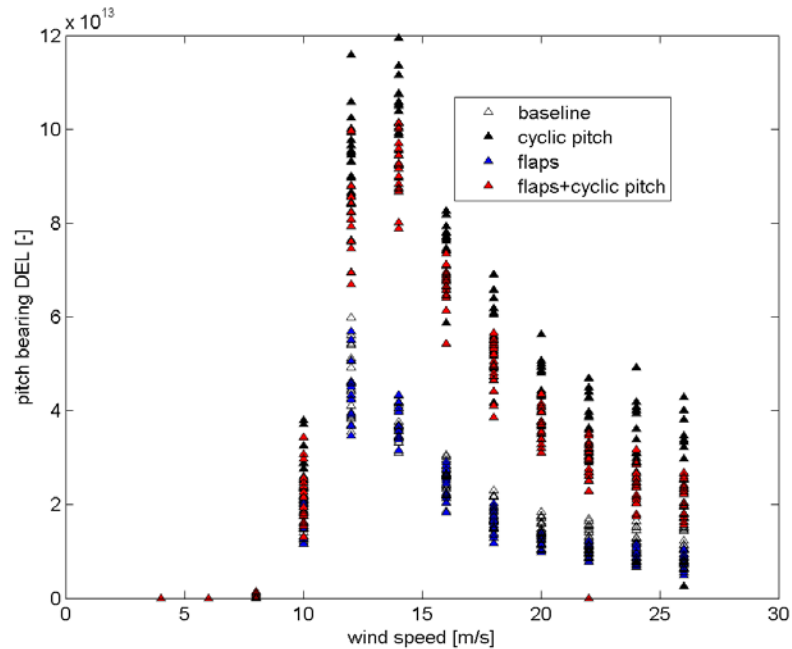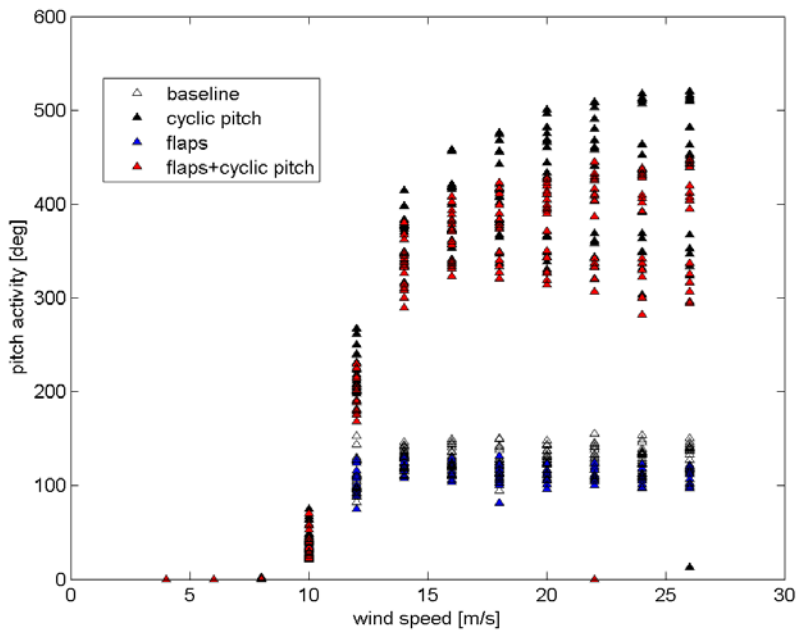

Figure 31 – Comparison pitch bearing short term fatigue equivalent loads between cases for DLC 1.2.

In **Figure 32**, the pitch activity in DLC 1.2 is shown for every wind speed, where all cases are compared and the similar trend is seen as in the case of the pitch bearing damage. It is seen that on average the individual pitch controls greatly increase the activity as expected, while the flap controls slightly decrease it (compared to the baseline) and the combined controls show a slight decrease compared to the individual pitch control.

Figure 32 – Comparison of pitch activity between cases for DLC 1.2.

In **Figure 33**, the flap activity in DLC 1.2 is shown for every wind speed, where all cases are compared. It is seen that there is an average increase in the flap activity in the combined case when compared to the flap only case.
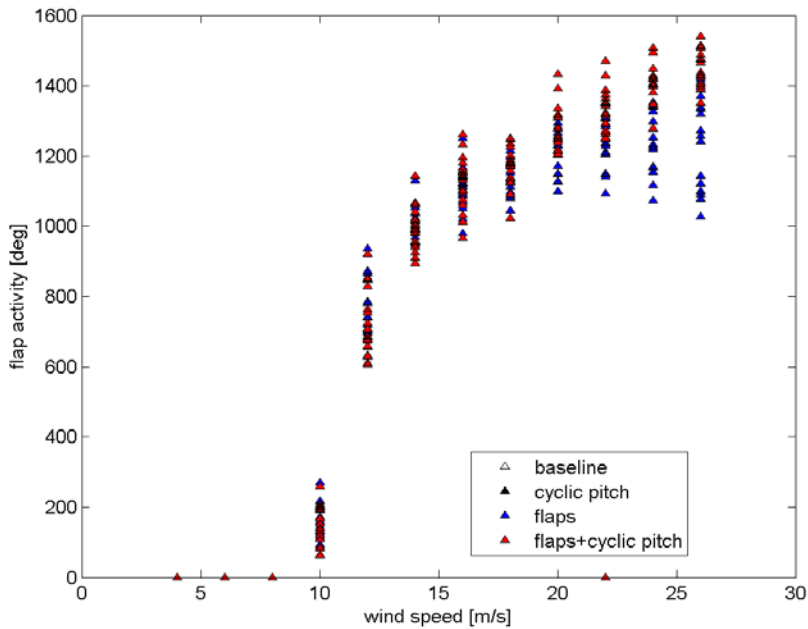

Figure 33 – Comparison of flap activity between cases for DLC 1.2.

In **Figure 34**, the power curve of every case is compared with average power binned over each wind speed. All load alleviation control concepts show no influence on average power

performance, as they are all designed to be mainly operational above rated power conditions. The impact on the Annual Energy Production (AEP) is minimal, a decrease of less than 0.25% is reported.
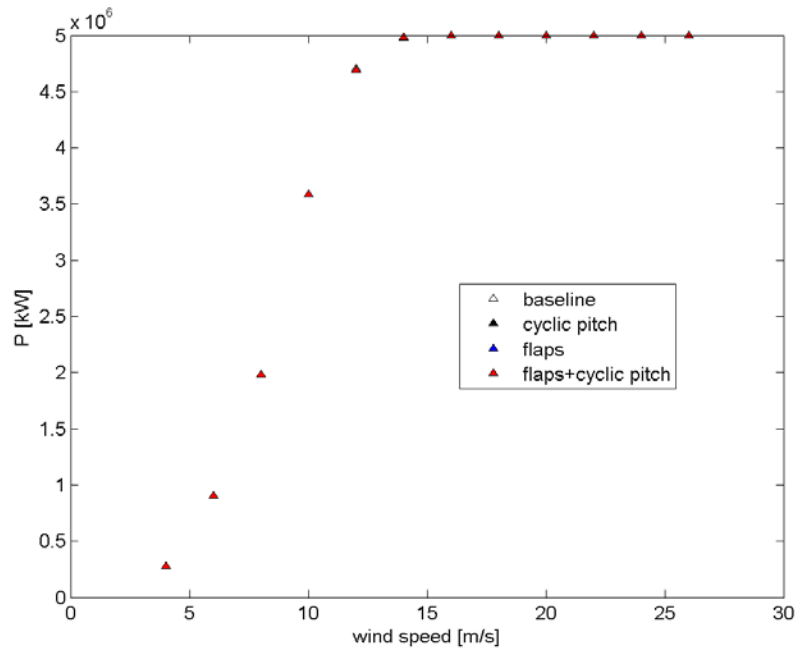

Figure 34– Comparison of average power curves between cases for DLC 1.2.

6. Conclusions

The three load control concepts (flaps, individual pitch, and combination of the two) have been evaluated in the full IEC-type of DLB revealing a realistic impact on design loads. The main conclusions of this study are summarized below:

- The individual pitch and flap controllers have a significant fatigue load alleviation impact on of blade, main bearing and tower loads, ranging from 2% to17%.
- The combined individual pitch and flap controller shows the best fatigue load alleviation performance, with alleviation up to 25 % on the blade root flapwise bending moment, around 7 % on the main bearings, and from 2% to 5% on the tower loads.
- Individual pitch control can increase fatigue loads in certain channels up to 5% (tower bottom side to side), whereas the flap activity increases the blade torsion fatigue loads by up to 10 % , 6% when combined with the individual pitch.
- The individual pitch controls increases the pitch activity and fatigue damage, while the flap and combined controllers decrease it compared to the baseline and to the individual pitch cases respectively.
- Individual pitch control can decrease extreme loads in certain channels up to 11%, while flap controls up to 11% and combined control up to 14%. The impact on extreme loads is very sensitive to specific controller parameters on fault cases.
- Individual pitch control increases extreme loads in certain channels up to 26%, while flap controls up to 11% and combined control up to 16%. The impact on extreme loads is very sensitive to specific controller parameters on fault cases.
- All cases show practically no impact on the AEP.

Suggested future work should focus on fine tuning of controllers for handling of extreme load cases, especially parked and fault cases, implementation of flaps on a more flexible and representative wind turbine model, and evaluation of advanced model-based combined controllers on the full DLB.

References

[1] Madsen, H. A., Andersen, P. B., Andersen, T. L., Bak C. and Buhl, T., The potentials of the controllable rubber trailing edge flap (CRTEF). Proceedings of EWEC 2010, Warsaw, Poland, 2010.

[2] Madsen, H. A. et al., Towards an industrial manufactured morphing trailing edge flap system for wind turbines, Proceedings of EWEC 2014, Barcelona, Spain, 2014.

[3] Barlas, T. K., Madsen, H. A. and Andersen, T. L., Design and simulation of the rotating test rig in the INDUFLAP project, DTU Vindenergi-E-0063(EN), 2014.

[4] Barlas, T. K., Madsen, H. A, Enevoldsen, K. and Klemmensen, K., flap testing on the rotating test rig in the INDUFLAP project, DTU Vindenergi-E-0064(EN), 2014.

[5] Barlas, T. K. and van Kuik, G. A. M., Review of state of the art in smart rotor control research for wind turbines, Progress in Aerospace Sciences — 2010, Volume 46, Issue 1, pp. 1-27, 2010.

[6] Hansen, M. H. et al., Design Load Basis for onshore turbines, Technical report, DTU Vindenergi-E-0174(EN), 2015 (to appear on orbit.dtu.dk).

[7] IEC. IEC 61400-1. Wind turbines – Part 1: Design Requirements, 2005.

[8] Verelst, D., prepost-wind-dlc INDUFLAP_v0.1, http://dx.doi.org/10.5281/zenodo.13370

[9] Pedersen, M. M., Post processing of Design Load Cases using Pdap, Technical report, DTU Vindenergi-I-0371(EN), 2014.

[10] Natarajan, A. and Holley, W. E., Statistical Extreme Loads Extrapolation with Quadratic Distortions for Wind Turbines, ASME Journal of Solar Energy Engineering, Vol. 130, 031017, Aug 2008

[11] Jonkman, J. et al., Definition of a 5-MW reference wind turbine for offshore system development. Technical report, NREL/TP-500-38060, 2009.

[12] Larsen, T. J. et al., How 2 Hawc2, the user's manual, Technical report, Risø-R-1597(ver. 4-4)(EN), 2013.

[13] Bergami, L., Adaptive Trailing Edge Flaps for Active Load Alleviation in a Smart Rotor Configuration, PhD thesis, DTU Wind Energy, 2013.

[14] Bergami, L. and Gaunaa, M., ATEFlap Aerodynamic Model, a dynamic stall model including the effects of trailing edge flap deflection, Technical report, Risø-R-1792(EN), 2012.

[15] N. N. Sørensen. General purpose flow solver applied to flow over hills. Technical Report Risø-R-827(EN), 1995.

[16] Hansen, M. H. et al., Basic DTU Wind Energy controller, Technical report, DTU Vindenergi-E-0018(EN), Edition 2, 2015 (to appear on orbit.dtu.dk).

[17] Bossanyi, E. A., Further load reductions with individual pitch control, Wind Energy, 8 (4): 481-485.

[18] Hansen, M. H., Aeroelastic stability analysis of wind turbines using an eigenvalue approach, Wind Energy, 7:133-143, 2004.

[19] \\mimer\hawc2sim\NREL5MW\C0032\res\C32_LoadRep.docx

[20] \\mimer\hawc2sim\NREL5MW\C0037\res\C37_LoadRep.docx

[21] \\mimer\hawc2sim\NREL5MW\C0034\res\C34_LoadRep.docx

[22] \\mimer\hawc2sim\NREL5MW\C0035\res\C35_LoadRep.docx

Load alleviation potential of the Controllable Rubber Trailing Edge Flap (CRTEF) in the INDUFLAP project

Acknowledgements

DTU Wind Energy is a department of the Technical University of Denmark with a unique integration of research, education, innovation and public/private sector consulting in the field of wind energy. Our activities develop new opportunities and technology for the global and Danish exploitation of wind energy. Research focuses on key technical-scientific fields, which are central for the development, innovation and use of wind energy and provides the basis for advanced education at the education.

We have more than 240 staff members of which approximately 60 are PhD students. Research is conducted within nine research programmes organized into three main topics: Wind energy systems, Wind turbine technology and Basics for wind energy.